Department of Electrical and Computer Engineering

Optimal Dispatch of Shunt Capacitors and Load Tap Changers in Distorted Distribution Systems using Ant Colony Algorithms

Sara Deilami

This thesis is presented for the Degree of
Master of Philosophy
of
Curtin University

November 2010

Declaration

To the best of my knowledge and belief this thesis contains no material previously published by any other person except where due acknowledgment has been made.

This thesis contains no material which has been accepted for the award of any other degree or diploma in any university.

Signature: ……S.Deilami…….

Date:……30.11.2010……...

ABSTRACT

This thesis investigates the performances of a class of intelligent system algorithms in solving the volt/VAr/THD control problem for large distribution systems. For this purpose, optimal dispatch of Load Tap Changers (LTCs) and Switched Shunt Capacitors in distribution networks with high penetration of nonlinear loads is studied. The optimization problem consists of determination of LTC positions, switched shunt capacitors statuses and proper coordination of these switched elements such that power loss is minimized, voltage profile is improved and total harmonic voltage distortion (THDv) is acceptable while network and operational constraints are satisfied. The Decoupled Harmonic Power Flow (DHPF) is employed for solving the optimization problem. In the next step, an Ant Colony algorithm (ACA) is developed and implemented as an effective and new technique to capture the near global solution of the dispatch problem. Simulation results based on ACA, Genetic Algorithm (GA) and Fuzzy-GA are presented and compared to show the accuracy of the proposed approach. Finally, the application of the developed dispatch ACA in smart grids with Plug-In Electric Vehicle (PEV) charging activities in the residential networks is considered. ACA is first applied on the distribution part of the smart grid to minimize losses, improve voltage profile and mitigate harmonic distortions. Then, a smart load management (SLM) algorithm is proposed and tested for the coordination of PEVs on the residential feeders. The developed algorithm is tested on smart grid configuration with 449 buses consisting of the IEEE 31-bus distribution system connected to a number of low voltage residential feeders populated with PEVs. Simulation results are presented and compared for uncoordinated (random) and SLM coordinated PEV charging considering consumer designated priorities and charging zones.

ACKNOWLEDGMENTS

I am heartily thankful to my supervisor, Associate Professor Mohammad A.S. Sherkat Masoum, whose encouragement, supervision and support from the preliminary to the concluding level enabled me to develop an understanding of the subject and completion of my thesis. It is a pleasure to thank my chair and co-supervisor, Professor Syed Islam and Dr. Ahmed Abu-Siada for their advices, supports and guidance throughout my research. I would also like to express my gratitude to Dr. Masoum's HDR (higher degree by research) group at Curtin University for their contribution, help and support during the completion of the project.

I also offer my regards and blessings to my beloved family who gave me their inseparable moral support, encouragement and prayers to the end of my education. Finally, I would like to express special appreciation to my husband for his endless dedication, love and patience throughout the completion of my MS thesis.

TABLE OF CONTENTS

LIST OF FIGURES

LIST OF TABLES

CHAPTER ONE

INTRODUCTION

In recent years significant research has been carried out proposing intelligent systems applications in the optimization of losses and regulation of voltage magnitudes in large distribution systems. More recently, [1-2] have also focused on obtaining similar solutions incorporating nonlinear loads. The key reason for the popularity of intelligent system approaches have been their ability to handle large and complex power systems including nonlinearities as opposed to analytical solutions. The intelligent algorithms namely GA and GA-Fuzzy [1-2] have been proven to provide much better results in comparison to base level solutions with no optimizations.

The operation of distribution system depends on the type, location and duration, as well as demand time and level of the electricity load. Load variation may lead to severe problems in distribution system such as voltage violation and intensification of power loss [1-3]. It can result in various operational problems such as high system losses, unacceptable voltage profile and inadequate electricity demand. The conventional solution consists of scheduling Load Tap Changer (LTC) and switched shunt capacitors to optimize system performance. The objective of the planning is to keep the voltage within the preset limits under changing load conditions while minimizing power losses.

With the extensive application of the present and future industrial and residential loads such as large variable- speed drives, charging stations, plug-in electric vehicles, smart appliances and home area networks, it is essential to improve the objective planning and accurately perform the scheduling in the presence of harmonics.

This thesis investigates the performances of a class of intelligent system algorithm in solving the volt/VAr/THD_V control problem for large distribution systems. Two dispatch optimal solutions based on genetic algorithm (GA) and ant colony algorithm (ACA) are implemented in Matlab. The algorithms are tested on various IEEE distribution systems and a 449 node smart grid configuration with residential feeders populated with plug-in electric vehicles (PEVs). A relatively fast and accurate

decoupled harmonic power flow algorithm is employed and utilized as the backbone of the optimization [1, 4].

The proposed evolutionary ACA is based on various aspects of the ants' behaviour and constitutes some Meta heuristic optimizations [6] which have been applied for various problems and systems. ACA considers load variations over a 24-hour period, includes harmonic voltage distortions and is applied to solve the dispatch problem using coordinated switching of LTC and shunt capacitor banks. A second ACA is also developed and utilized to determine the optimal load interval division of the daily load curves.

In order to investigate and compare the performances of the genetic and AC based techniques, simulations will be performed for the following systems:

- The IEEE 31-bus system with multiple nonlinear loads that injects current harmonics to the system. Simulations will be carried out for sinusoidal and non-sinusoidal conditions.
- The IEEE 123-bus system with a number of nonlinear loads having different V-I characteristics [1].
- A 449-bus smart grid configuration consisting of a distribution system connected to a number of residential feeders with multiple PEV charging activities [5].

The last part of the thesis presents a smart load management (SLM) approach for the coordination of PEV charging to minimize system losses and regulate voltage magnitudes at all buses. The proposed SLM is demonstrated on the IEEE 31-bus system. This is done after performing optimal dispatch of LTC and switched capacitors using ACA.

A comparison between GA and ACO was performed in terms of computation time and number of generations required to capture the near-global optimal solution.

Detailed simulation results show that the two intelligent algorithms perform better than ad-hoc placement of reactive power sources but differ in convergence, computational effort and accuracy of solution. It is hoped that the results presented in this thesis will help consolidate the research directions in this area of distribution system optimization using intelligent algorithms.

1.1. Research Objectives

The main objective of this research is to investigate the optimal dispatch of LTC and switched shunt capacitors while taking harmonics into account. The specific objectives of the study are as follows:

1. Formulation of the optimal problem and selection of required constraints (i.e., voltage, THD_V, and number of capacitor switching) for the placement and sizing of shunt capacitor banks in radial distribution networks in the presence of voltage and current harmonics.
2. Investigation of influence of harmonics on optimal dispatch scheduling.
3. Application of genetic algorithm (GA) for the problem of optimal dispatch of LTC and shunt capacitor.
4. Investigation of performance of the novel ant colony optimization approach and development of an AC based dispatch solution in the presence of harmonics [6].
5. Comparison of GA and AC solutions in terms of accuracy and computing times.
6. Educated recommendations based on the results and discussions.
7. Dissemination of outcome of research on conferences and journals, and ultimately in this Master thesis.

1.2. Thesis Contributions

In this study, optimal dispatch of LTC and switched shunt capacitors under non-sinusoidal operating conditions is considered as the optimization problem. In regards to the complexity and large problem dimension, a new evolutionary based ACA is proposed and implemented to efficiently solve the problem. Results are compared with those generated by GA and the importance of harmonics are thoroughly studied and discussed.

1.3. Thesis Outline

This thesis is organized in seven chapters. Chapter 2 presents an introduction to large distribution networks and optimization problems. It emphasizes the importance of implementing new effective techniques for optimal dispatch of LTC and shunt

capacitors. In addition, the application of LTC and shunt capacitors and their effective roles simultaneously minimizing system losses, improving voltage profiles and mitigating harmonic distortions are highlighted. Chapter 3 investigates a relatively new and emerging optimization tool based on the behaviour of ants and their abilities to select the best search paths. Ant colony optimization is reviewed and its application and effectiveness in capturing near-global solutions is discussed. Chapter 4 presents a comprehensive study and review on genetic optimization. Chapter 5 consists of all the simulation results performed for optimal scheduling of LTC and shunt capacitors. Simulations are based on generated optimal scheduling and show an efficient comparison between ACO and GA solutions. Chapter 6 considers the application of ACA in smart grids with PEV charging activities in the residential feeders. ACA is first applied on the distribution part of the smart grid to minimize losses and improve voltage profile and the quality of power. Then, a smart load management (SLM) algorithm is proposed and tested for the coordination of PEVs on the residential feeders. Conclusion and recommendations for future research directions are presented in Chapter 7.

CHAPTER TWO

OPTIMAL DISPATCH OF LTC AND SWITCHED SHUNT CAPACITORS IN DISTORTED DISTRIBUTION SYSTEMS

Distribution systems are becoming more complicated and require continuous enhancement. Most existing systems are under stress and need reinforcing and upgrading. High performance and reliability are essential factors in distribution system and the emerging smart grid configuration. The operation of distribution system depends on the type, location and duration, as well as demand time and level of the electricity load. Load variation may result in various operational problems such as high system losses, unacceptable voltage profile and inadequate electricity demand [1-3]. The conventional solution consists of scheduling Load Tap Changer (LTC) and switched shunt capacitors to optimize system performance. The objective of the planning is to keep the voltage within preset limits under changing load condition while minimizing power losses.

2.1. Literature Review on Optimal Dispatch

The growing demand for electricity and the problems associated with load variations can be satisfied by careful system planning. The objective of distribution system planning is to employ simple, economical and effective approaches to satisfy the growing demand for electricity. The challenging issue has been the dynamic nature of the industrial and residential loads that must be carefully monitored and compensated to achieve acceptable efficiency and voltage profiles over a 24 hour period. Otherwise, the change of electricity demand may cause operational problems in distribution systems such as voltage violation and power loss escalation. The widely accepted strategy [1] essentially consists of optimal dispatch of the controllable devices such as LTC, shunt reactors and switched shunt capacitors installed on substation and feeders.

A LTC is usually placed at the secondary side of the substation transformer to control the substation secondary voltage and regulate the bus voltages under changing load conditions [7-9]. This is not an effective approach as the LTC can only

set the voltage level by changing the level of secondary bus voltage. It will not significantly improve the feeder's voltage profile. A better approach to improve the voltage profile is to inject reactive power by installing shunt capacitor banks on secondary side substations and feeders during the peak - load hours [8, 9]. The capacitors must be switched off during light-load conditions. The ultimate solution is the simultaneous control and coordination of the two switching devices in order to effectively improvement voltage profile and decrease system power losses over the 24 hour period [10, 11]. This is a complicated process that requires optimal dispatch and scheduling of the LTC and switched shunt capacitors.

The optimal dispatch of LTC and switched shunt capacitors is a multi-phase decision-making problem with discrete (integer) variables and nonlinear objective function [12, 13]. It is a difficult, timely and tedious optimization problem to tackle due to the following facts:

- The nonlinear dependency of the bus voltage to the LTC position and capacitor statuses [14, 15].
- Secondary bus voltage are required to determine the status of shunt capacitors [12]. This is to ensure that the bus voltages will remain within the allowable limits after the switching actions.
- Interaction and reliance between the controllable devices [8, 11, 15-19].
- The interaction between the switchable components causes oscillations in the controllable devices.
- The LTC problem depends on the shunt capacitor status since their statuses must be determined prior to tap changing [19].
- The switching effects of shunt capacitors on secondary bus voltage may cause additional LTC tap position changes, which forces LTC to operate too frequently resulting in reduction of LTC lifetime and higher maintenance cost.
- The near-global solutions must be attained in the least possible number of control steps [14].
- The large dimension optimization problem requires extensive computing time since the power flow calculations and scheduling must be performed on hourly

basis over the 24 hour period [20]. This will be an issue for optimal dispatch of large interconnected power system based on nonlinear iterative optimization approaches.

- The maximum switching of the control devices needs to be checked as they are limited for a specific switching schedule. This will cause more complexity as switching limits need to be checked for all possible solutions [20].

Initially, a number of approaches were adopted to simplify the optimal dispatch problem, including:

- Independent operation of LTC and shunt capacitors for separate control of the voltage and reactive power [8].
- Defining shunt capacitors status prior to determining the LTC status [10, 11, 17, 18, 21, 22].
- Assuming a single voltage level condition [23].
- Dividing the problem into two sub-systems and using different techniques to separately solve them [24, 25]. This will provide a local (not global) optimal solution as the interaction between two sub-systems is not considered.
- The constrained optimization problem is simplified using the corresponding unconstrained solution [26]. The constraints are check after the unconstrained problem is solved and the invalid solutions are discarded. This approach may converge to a local solution.
- The solution of the unconstrained problem is used as the initial condition for the constrained optimization problem to reduce required computing time [26].

Ultimately, an accurate solution to the nonlinear dispatch problem is achieved by defining a multi-phase decision-making constraint optimization problem with discrete variables that simultaneously controls LTC and switched shunt capacitors to minimize the objective function (e.g., system losses over the 24 hours period) and improves voltage profile while satisfying the operational constraints.

2.2. Impact of Nonlinear Loads and Harmonic Distortions of the Optimal Dispatch Problem

There are growing concerns and issues about the harmonic distortions associated with power system equipment (e.g., saturated power transformers), devices (e.g., regulators and Flexible Alternative Current Transmission System (FACTS) controllers), nonlinear loads, and distributed renewable energy resources (photovoltaic, wind power and micro grids). There are also concerns about the impact of some nonlinear loads such as large PEV charging stations and individual PEV battery chargers on the overall daily load pattern of distribution systems [27]. As the applications of nonlinear loads are increasingly becoming popular, special attention should be paid to the optimal dispatch problem in such distorted systems. This is due to increased losses, extensive reactive power demand, over-voltages at fundamental and harmonic frequencies and possibility of harmonic resonances.

With the extensive application of the present and future industrial and residential loads such as large variable-speed drives, charging stations, plug-in electric vehicles, smart appliances and home-area networks, it is essential to improve the objective planning and accurately perform the scheduling in the presence of harmonics. Recent research has shown that disregarding harmonic currents and voltages will lead to unacceptable results due to increased distortion levels and additional power losses [1-3, 27-32]. However, considering harmonics in realistic large distribution systems with many nonlinear loads will significantly complicate the scheduling problem, influence the optimization procedure [1, 2] and may generate different local (not global) results.

Recent research has shown that disregarding harmonic currents and voltages will lead to unacceptable results due to increased distortion levels and additional power losses [1-2]. Several optimization programs have been introduced for power loss reduction and voltage regulation by allocating shunt capacitors considering harmonics [23]. However, they were carried out for single-load-level conditions without LTCs. In recent years, new optimization methods such as Fuzzy- Logic (FL) and Genetic Algorithm (GA) have been performed for global optimization problems [1, 2, 23, 27-32]. These evolutionary-based algorithms offer new optimization

techniques for finding the global optimal solution. With some approaches such as GA, the computation time and number of iterations will need to be significantly increased to achieve more accurate results. Many methods are also unable to handle the discrete nature of an optimization problem.

A relatively new and promising near-global optimization approach for multi-phase decision-making problems with discrete variables and nonlinear objective functions is the Ant Colony Optimization (ACO) [33-39]. It is based on various aspects of the ants' behaviour and constitutes some Meta-heuristic optimizations. Meta-heuristic designates a computational method that optimizes a problem by iteratively trying to improve a candidate solution with regard to a given measure of quality. Ants start their search for finding food sources from their destination (nest) and choose a different combination of paths. They are capable of communicating in their colonies by depositing a chemical secretion and some heuristic information. Ant Colony algorithm (ACA) was introduced and developed by Dorigo in 1992 [6, 33]. Various versions of ACA have been developed to improve its performance based on the nature and complexity of the applications [34-38].

In order to include the impact of nonlinearity in the optimal dispatch and scheduling of LTC and shunt capacitors, a harmonic load flow algorithm is required. The algorithm will be used as the backbone of the optimization problem to compute voltage and current harmonics, harmonic losses and the total harmonic distortion (THD). It is argued that considering harmonics in realistic large distribution systems with many nonlinear loads will lead the planning to be very complicated and will significantly influences the optimization solutions [28, 29]. It may also reduce the optimization benefits [23]. Harmonic power flow calculation is more complicated than the conventional power flow calculation and requires extensive computer memory and computing time.

2.3. Decoupled Harmonic Power Flow (DHPF)

Harmonic power flow algorithms are divided into two general classes:

- Coupled harmonic power flow (HPF) [28-29] with accurate modeling of nonlinear loads including the dependencies and couplings between all harmonics, i.e. the harmonic voltage at each frequency (e.g., V^5) depends on the magnitude and

phase angle of current at other harmonics (e.g., I^{1}, I^{5}, I^{7}, I^{11}, I^{13} etc.). HPF algorithms are very accurate; however, they require long computing times and are not suitable candidates for the optimal dispatch problems that are usually solved using nonlinear iterative procedures.

- Decoupled harmonic power flow (DHPF) where the couplings between harmonics are not considered and nonlinear loads are modeled as harmonic current sources with associated (estimated, computed or measured) magnitudes and phase angles. DHPF algorithms are relatively fast with good convergence characteristics. According to [1], DHPF have acceptable accuracy compared to HPF.

Most references [1, 40- 42] and commercial software packages (such as Electrical Transient Analyser Program (ETAP)) use a decoupled approach for the harmonic load flow formulation. DHPF is widely used and accepted for planning and optimization of large power system since the memory storage, computation time and speed are very essential in capturing the global solution. Most optimization algorithms (including GA, GA-Fuzzy and ACA) require many executions of harmonic power flow calculations. The main advantage of the few available coupled HPF algorithms (such as HARMFLOW [3 ,42]) is their high accuracy in modelling the coupling between harmonics coordinated by the nonlinear loads.

This thesis uses the developed DHPF of [2, 4]. Nonlinear loads are modelled as the combination of passive elements and current sources at higher frequencies [40]. Linear load are modelled as resistances in parallel with inductances at the fundamental frequency to represent the active and reactive power, respectively [40,41]. Nonlinear loads are modelled by ideal harmonic current sources injecting harmonic currents injected to the distribution system [4, 40]. The harmonic current sources are used to determine voltage waveform characteristics and additional losses at harmonic frequencies.

At harmonic frequencies, the distribution system is modelled by a harmonic admittance matrix and harmonic current sources. The harmonic bus admittance matrix is constructed using the component models as follows:

- The admittance matrix $Y^{(h)}$ representing the system at harmonic frequency is computed by modifying the conventional fundamental admittance according to the harmonic order:

  $Y_{jj}^{(h)}$ = main-diagonal entries= sum of line admittances connected to bus j (j = 1, …, n) at the h^{th} harmonic frequency.

  $Y_{jk}^{(h)}$ = off-diagonal entries= - (line admittance connected between buses j and k at the h^{th} harmonic frequency).

- The distribution lines are represented as lumped parameter elements connected in a nominal-π configuration. The shunt ($y_{line,\ shunt}^{(h)}$) and longitudinal ($y_{line,\ longitudinal}^{(h)}$) parameters of the lines are included in the diagonal and off-diagonal entries of the admittance matrix $Y^{(h)}$, respectively:

$$y_{line,\ longitudinal}^{(h)} = y_{i,i+1}^{(h)} = \frac{1}{R_{i,i+1} + j2\pi h L_{i,i+1}} \tag{2-1a}$$

$$y_{line,\ shunt}^{(h)} = y_{i,i}^{(h)} = y_{i+1,i+1}^{(h)} = \frac{1}{j2\pi h C_{i,i+1}} \tag{2-1b}$$

  where $R_{i,i+1}$, $L_{i,i+1}$ and $C_{i,i+1}$ represent the resistance, reactance and capacitance of the line segment between busses i and $i+1$, respectively.

  Overhead distribution lines have small line capacitances that are not usually considered in the admittance matrix. However, distribution cables have relatively high per-phase line to ground capacitances that must be included in $Y_{ii}^{(h)}$ entries.

- The general model of linear load as a resistance in parallel with a reactance is utilized. The admittance of the linear load connected at bus i is defined as:

$$y_{linear,\ i}^{(h)} = \frac{P_{linear,\ i}}{\left|V_i^{(1)}\right|^2} - j\frac{Q_{linear,\ i}}{h\left|V_i^{(1)}\right|^2} \tag{2-2}$$

where $P_{linear,\,i}$ and $\boldsymbol{Q}_{\boldsymbol{linear,\,i}}$ are the respective active and reactive linear loads at bus *i* and $V_i^{(1)}$ is the fundamental voltage at bus *i* obtained from the fundamental power flow calculations. Superscript 1 corresponds to the fundamental frequency.

Shunt capacitor banks are represented as shunt connected elements:

$$y_{capacitor,\,i}^{(h)} = h y_{capacitor,i}^{(1)} \tag{2-3}$$

where $y_{capacitor,\,i}^{(1)}$ is the admittance of shunt capacitor *C* at bus *i.*

- Nonlinear loads are modelled as decoupled harmonic current sources that inject harmonic currents into the system. The fundamental and the h^{th} harmonic currents of the nonlinear load installed at bus *i* with real power P_{ni} and reactive power Q_{ni} are [12]:

$$I_i^{(1)} = \left[\left(P_{ni} + jQ_{ni}\right)/V_i^{(1)}\right]^* \tag{2-4}$$

$$I_i^{(h)} = C(h) \times I_i^{(1)} \tag{2-5}$$

where *C(h)* is ratio of the h^{th} harmonic current to its fundamental current and * is complex conjugate.

A conventional Newton-Raphson algorithm is used to solve power flow at fundamental frequency and harmonic voltages are calculated by solving the following load flow equation, which is derived from the node equations [42]:

$$Y^{(h)}V^{(h)} = I^{(h)} \tag{2-6}$$

where $Y^{(h)}$, $V^{(h)}$ and $I^{(h)}$ are the bus admittance matrix (Eq. 2-1), the bus voltage vector and the bus injection currents (by nonlinear loads) at the h^{th} harmonic order, respectively.

At bus *i*, the *rm*s value of the voltage and the Total Harmonic Distortion of voltage (THD_{vi}) are defined as:

$$V_{irms} = \left(\sum_{h=1}^{H} \left| V_i^{(h)} \right|^2 \right)^{1/2} \tag{2-7}$$

$$THD_{vi} = \frac{\left(\sum_{h \neq 1}^{H} \left| V_i^{(h)} \right|^2 \right)^{1/2}}{\left| V_i^{(1)} \right|} \times 100\% \tag{2-8}$$

where H is the highest harmonic order considered.

At the h^{th} harmonic frequency, power loss in the line section between busses i and $i+1$ is expressed below [12].

$$P_{loss(i,i+1)}^{h} = R_{i,i+1} \left(\left| V_{i,i+1}^{(h)} - V_i^{(h)} \right| \left| y_{i,i+1}^{(h)} \right| \right)^2 \tag{2-9}$$

The total power loss, including losses at harmonic frequencies, for an n bus system is:

$$P_{loss} = \sum_{h=1}^{H} \left(\sum_{i=1}^{n} P_{loss(i,i+1)}^{(h)} \right) \tag{2-10}$$

The accuracy of the harmonic power flow algorithm greatly contributes to the precision of the optimization results.

2.4. Conclusion

As discussed in this chapter, extensive and comprehensive researches have been implemented to investigate the possible solutions in distribution systems in terms of voltage profile improvement and power losses reduction. In recent years, a number of researches have been focused on employing control devices such as LTC and switched shunt capacitors to solve the problem of power losses escalations and voltage violations. For optimal dispatching, a typical daily load curve has been considered and used for linear and nonlinear loads.

In addition, power quality of distribution systems and its impact on the optimal dispatch solution have also been investigated in recent literature. Published documents indicate that nonlinear loads and the associated harmonic voltage and current distortions will definitely complicate the optimization procedure and affect the solutions. In the following chapters, two intelligent optimization approaches based on GA and ACA will be presented and applied to the dispatch problem.

CHAPTER THREE

PROPOSED ANT COLONY ALGORITHM FOR OPTIMAL DISPATCH OF LTC AND SHUNT CAPACITORS

This chapter proposes for the first time an ant colony algorithm (ACA) for optimal dispatch of LTC and shunt capacitors in the presence of harmonic currents and voltages caused by nonlinear loads. ACA has been recently (2007) implemented for the optimal dispatch problem under sinusoidal conditions [38]. One of the contributions of this research is the implementation and testing of ACA under non-sinusoidal operating conditions considering nonlinear loads. The DHPF of Section 2.3 is used as the backbone of the ACA. This chapter outlines the AC optimization concepts, formulation and flow chart. Simulation results for the optimal scheduling of LTC and switched shunt capacitors using the proposed ACA and the GA (Chapter 4) are presented and compared in Chapter 5. The new ACA is relatively faster than GA and can capture the near-global optimal solutions of the multi-phase decision-making problems with discrete variables and nonlinear objective functions. A thorough investigation and review of the subject has been performed and will be presented in the following sections.

3.1. Ant Colony Algorithm (ACA)

Several optimization algorithms have been introduced for power loss reduction and voltage regulation by allocating fixed and switched shunt capacitor banks considering harmonics [23, 30-32]. These evolutionary-based algorithms offer new optimization techniques for finding the near-global optimal solutions. One of the best and most popular recent methods is ant colony optimization (ACO). This novel technique is introduced as a probabilistic approach for solving computational problems to find proper solutions (paths) through graphs. The ant colony algorithm is a member of swarm intelligence methods based upon some Meta heuristic optimizations [6]. ACA was first introduced and developed by Dorigo in 1992 [6, 37] in his PhD Thesis. The idea of ACO is based on the behavior of ants and target discrete optimization problems [34]. This technique was initially utilized to investigate an optimal path between ant colonies and source of food. Various search

graphs were established for this investigation. This idea has been extended to solve wide variety of problems in different areas and for different applications such as quadratic assignments, travelling problems and vehicle routing, as well as, communications, control and power system [38]. The application of ACO in power system has mainly focused on optimal generation scheduling [38, 39] and optimal reactive power dispatch [38]. Different versions of ACA have also been developed to improve its performance based on the nature and complexity of the applications [37-39].

3.1.1. Basic Concept of Ant Colony

Generally, ACO has been inspired by the behavior of real ant colonies [6, 34]. This promising optimization approach is based on the fact that ants are capable of finding the shortest path from food sources to the nest without using visual cues [6].

Ants are part of the social insects that live in colonies. Actual ants are totally blind. They communicate between their colonies based on the simple mechanism [38] of depositing a chemical substance trail, called pheromone on the ground when they move. Therefore, they rely on the environment as a medium of communication. The deposited pheromone is then observed by other ants and with some heuristic information motivates them to follow the path with a high probability [37]. The probability of a path will increase as more ants choose the same path since the deposited pheromone trails will be added up which will lead to a food source closer to the nest. On the other hand, if some paths are not popular they will eventually be isolated as the pheromone evaporates over time resulting in less attraction on certain paths. Therefore, some groups of ants may choose the same path with no pheromone trail as shown in Fig. 3.1. The evaporation process enables the group of ants to forget bad decisions previously made by some ants.

Basically, in case of having the same quantity of pheromone on all edges over the time, no paths would be chosen. However, there is a feedback which causes a slight variation on the path (edge) and thus that path is allowed to be selected. This will lead the algorithm to change its status from an unstable situation when all the solutions are the same to a stable state with the strongest solutions.

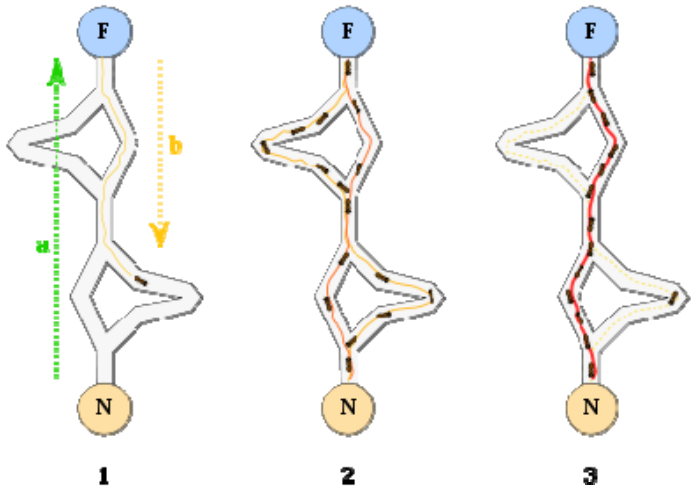

Fig. 3.1. An example of capturing the optimal path by real ants; (1) Ants follow a path between points F and N. (2) An obstacle is interposed; ants can choose to go around it following one of the two different paths with equal probability. (3) More pheromone is laid down on the shorter path.

3.1.2. Ant Colony Optimization Procedure

ACO is based on the above-mentioned behaviour of real ants to achieve the best solution. Generally, ACO starts with constructing a graph showing all possible search paths to be completed by the ants [38]. This search graph can be represented by the number of all nodes that will be visited including and the existing solution paths. At each step, ants select one possible solution at one node and step- by- step, build the entire graph. In this process, ants start their tour from one starting point (node) and select all the possible paths to reach their destination.

To start the search, it is important to assign an initial amount of pheromone and some related information (parameters). At each step, ants choose the next nodes based on the amount of pheromone trails and some heuristic information. Therefore, the paths with higher probabilities will be selected. This procedure involves the selection and behavior of the colony of ants throughout the various possible paths (search graph) which are affected by two local decision features: pheromone trails and attractiveness. Based upon this policy, each ant will add a solution to the problem. Upon the completion of a solution (tour) by each ant or during the construction phase, solution evaluations and pheromone modifications will be performed based on the defined fitness function of the optimization problem. The updated pheromone will direct and modify the search of the future ants. Furthermore, pheromone

evaporation and daemon actions will reduce the possibility of getting stuck in local optima. The daemon actions are used to bias the search process from a non-local perspective. The general procedure of the ACO algorithm is described in the following sections:

(A) Search Graph

In ACO, a search graph is required to be constructed in order to solve the optimization problem. Starting the optimization necessitates devising a construction graph which will be used by the colony of the ants throughout the process. All of the allocated ants for the problem are required to complete their tours by travelling the fully construction graph before jumping over to the next generation (Fig. 3.2). This graph can be shown as G(C, L), where C demonstrates the number of vertices (nodes) and L is a set of edges (arcs of the graphs).

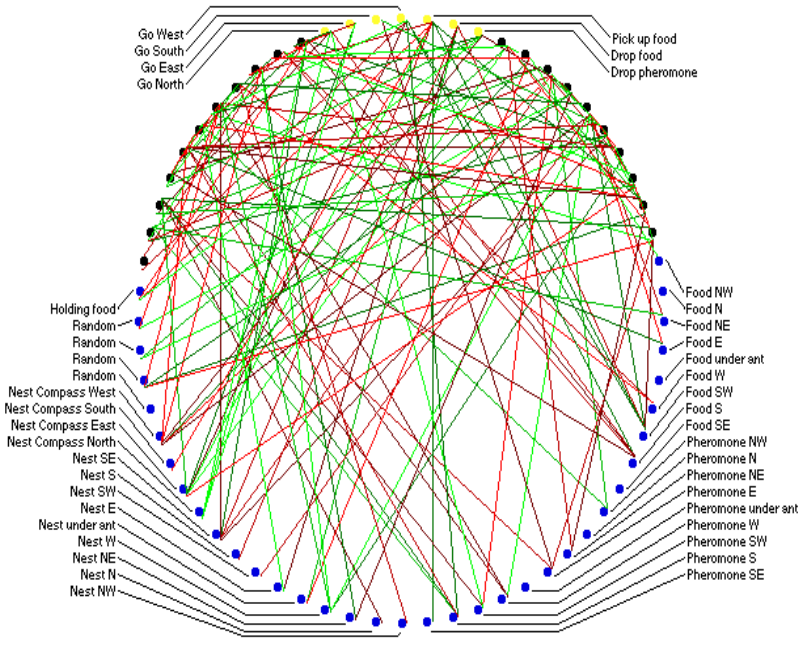

Fig. 3.2. Construction graph of G(C, L)

According to [37], this graph is obtained based on the set of solution components C in two different ways: they can be represented by edges or vertices. Each ant then travels from the nest (starting point) and moves along the edges to reach its destination. Therefore, a set of artificial ants create solution from the available paths in the construction graph. Constructing one solution by an ant starts from a partial

solution and at each step; this will be extended by adding set of feasible solutions which are safe in terms of constraints' violations. [37].

(B) Initialization

Initialization is an important step of the optimization process. It has been argued that ACO control parameters and initial pheromone setting has a significant influence on the performance of the optimization. When the search graph is constructed, all ants are positioned on their proper locations (starting point) and initial values for pheromone are considered for the search graph. Therefore, appropriate initial pheromone deposit needs to be defined for the ACA. This appropriate value may vary for different types of ACO. Typically, the value for the initial pheromone is more likely to be higher than the expected amount of pheromone deposited by the ants in one iteration. The initial value of pheromone (τ_0) is calculated by:

$$\tau_0 = m / f \tag{3-1}$$

where m is the number of ants and f is the estimated maximum value of the objective function.

This selection refers to the effects of this initial value on the outcome of the optimization problem:

- Low value of initial pheromone can force a quick decision making by the algorithm which may lead to premature convergence.
- For high value of initial pheromone instead, many iterations are lost waiting until pheromone values are adequately decreased by evaporation and the ants get the chance to add enough pheromone to bias the search. Therefore, it is crucial to select the proper initial pheromone value for each evolutionary algorithm.

(C) Tour Construction

After initialization and setting the initial amount of pheromone, the next possible solution is chosen based on the value of pheromone and some heuristic information. In this step, ants will deposit a certain amount of pheromone on either the edge or vertices of the graph which may be related to the captured solution. Obviously, ants prefer to move towards the solution (path) with high amount of pheromone. Eventually, ants will build their tour from starting point to their target. Then,

subsequent ants also use the pheromone information as guidance to next proper solution. At each step of the tour, a probabilistic rule is applied to detect the next possible solution. In other words, ant k at node i uses the probabilistic rule involving pheromone and heuristic information to move to node "j". The corresponding probability is calculated as:

$$p_{i,j} = \frac{(\tau_{i,j}^{\alpha})(\eta_{i,j}^{\beta})}{\Sigma(\tau_{i,l}^{\alpha})(\eta_{i,l}^{\beta})}, \quad j,l \in N(k,i) \tag{3-2}$$

where $\tau_{i,j}$ is the amount of pheromone on edge *i*,j; α is the parameter to control the influence of pheromone trail ; β is the parameter to control influence of $\eta_{i,j}$, and *N(k,i)* is the feasible neighbourhood of ant *k* when being at node *i*. Furthermore, $\eta_{i,j}$ is the heuristic information associated with node j (based on a priori knowledge). By this stochastic mechanism, the probability of choosing a particular solution increases with the value of the associated pheromone trail $\tau_{i,j}$ and the heuristic information value $\eta_{i,j}$. This heuristic information is defined as follows:

$$\eta_{i,j} = 1 / d_{i,j} \tag{3-3}$$

where $d_{i,j}$ is the distance between nodes i and j. The definition of the heuristic information may be totally different according to the optimization problem.
This process will finish after all ants complete their tour.

(D) Fitness Evaluation

Optimization problems usually require a fitness function to evaluate the solution domain. ACO also mandates defining a fitness function based upon the objective function of the optimization problem. Fitness function is provided to evaluate performance of the ants and also to control the progress of algorithm. Fitness function will also guarantee solution diversity and positive value of each individual's fitness.

After completion of the tour by all ants, the fitness value for each individual (ant) is calculated. The fitness evaluation is important in terms of classifying the existing solutions and selecting the optimal solution. In addition to the fitness function problem, constraints are also important and must be carefully defined. Constraints of an optimization problem may be checked in two different ways which has some

impact on the construction policy of the artificial ants. Depending on the optimization problem and related objective function, constraints are checked by accepting only feasible solutions created by ants. This is done by applying a penalty function for not feasible solutions.

After evaluating performance of all ants, the fitness values are used to update the amount of pheromone on the search graph for next iteration.

(E) Pheromone Update Process

Local Update Process: Once all ants have completed their tour, and before updating the pheromone, obtained solutions by ants may be updated applying a local search. This optional process depends on the type of ant algorithm being used. However, it is usually included in state-of-the-art ACAs. Upon the completion of each tour, each ant updates the local pheromone as follows [38]:

$$\tau_{i,j} = (1-\varphi)\tau_{i,j} + \varphi\tau_0 \tag{3-4}$$

where $\varphi \in [0, 1]$ and τ_0 are the decay coefficient and the initial value of the pheromone. The local Pheromone update rule is considered as an important step of the optimization algorithm. This updating process is assigned to increase the pheromone values related to the proper solutions and decrease the amount of pheromones associated with bad solution [37]. The pheromone value may be increased by adding good solutions or decreased through pheromone evaporation. In other words, pheromone evaporation is performed for the search group and will lower the amount of pheromones by the following calculation:

$$\tau_{i,j} = (1-\rho)\tau_{i,j} \tag{3-5}$$

where $0 < \rho < 1$ is the pheromone evaporation rate.

The pheromone evaporation is important to be considered as it avoids increasing the level of pheromones and helps the mechanism to forget bad decision of the past. Typically, updating process is performed at each iteration of the algorithm. This pheromone update may differ in different ACAs and will be discussed for each algorithm separately in the next sections.

(F) Convergence

Termination of the procedure is obtained if the number of iterations reaches the previously designated maximum value or the optimal solution is achieved. Furthermore, the algorithm will be terminated if all ants select the same tours or no improvement is found for a specific number of iterations.

3.1.3. The AC Optimization Algorithm

Basically, an objective function is defined for ant colony optimization. A specific formulation may be utilized for different optimization problems and therefore, different formulation and data structure are considered. According to abovementioned process, initializations are important to be taken into account. Moreover, aforementioned search graph is constructed to demonstrate the whole search space. After establishing input data, constructing the search graph and initial information for the related algorithm, ant colony system may be applied to the problem. This optimization process can be briefly described by the algorithm shown in Fig. 3.3.

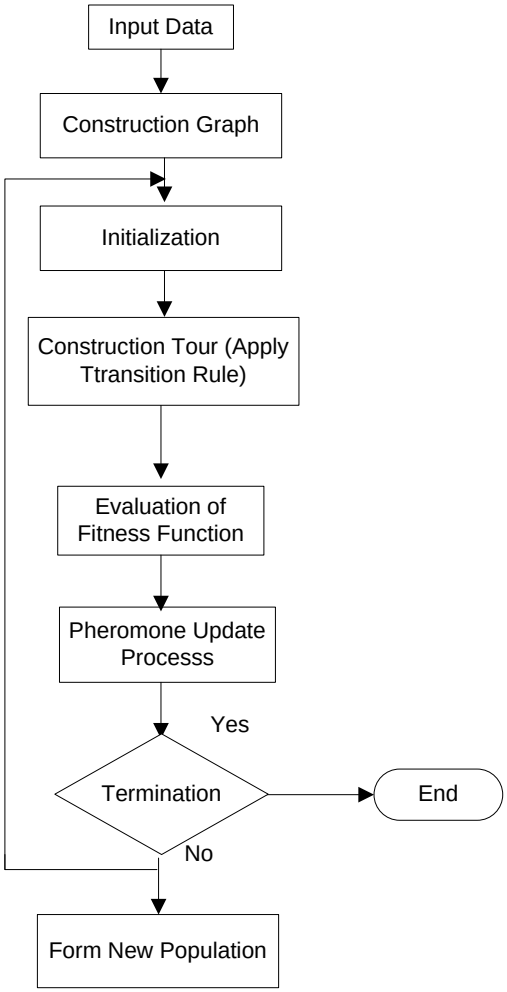

Fig. 3.3. General computation procedure of the ant colony algorithm

3.2. Main types of ACO Algorithms

Typically, different versions of ant colony algorithms have been developed to improve their performance based on the nature and complexity of the applications [37-39]. In the subsequent section, main ant colony algorithms will be introduced and discussions are made on their characteristics, advantages and disadvantages in solving different optimization problems.

3.2.1. Ant System (AS)

Ant system (AS) is the first proposed ACO algorithm which was aimed to solve the travelling salesman problem (TSP). The main goal was finding the shortest path to link a series of cities. It can be observed that the related algorithm is relatively simple using a selected number of ants to construct the possible paths along the cities. Reviewing this algorithm demonstrates some shortages comparing to the available

algorithms for TSP (travelling salesman problem). There are some main differences between the initially implemented AC and its improved generations in terms of the pheromone updating process and management of the pheromones. In AS, initial value of pheromone is defined slightly higher than the expected value of deposited pheromone in one iteration which is calculated by Eq. (3-1).

In this process, pheromones are updated by all ants which have their own possible solution in the iteration by Eq. (3-4).

After evaporation, all ants lay down pheromone on the paths based on the following formulation:

$$\tau_{i,j} = (1-\rho)\tau_{i,j} + \rho \Delta\tau_{i,j} \tag{3-6}$$

where $\Delta\tau_{i,j}$ is the amount of pheromone deposited, typically given by

$$\Delta\tau_{i,j}^{k} = \begin{cases} 1/L_k, & \text{if ant } k \text{ travels on edge } i,j \\ 0, & \text{otherwise.} \end{cases} \tag{3-7}$$

L_k is the value of the objective function related to the tour built with ant k. It can also be set to the path length based on the selected ant colony optimization technique. According to above formulation, pheromone values demonstrate the quality of the tours constructed by the ants. More pheromone value specifies better solution. Generally, best tours refer to the proper solutions with shorter distances and more pheromone value and therefore, they are more likely to be selected by ants in next iterations in the optimization algorithm [38].

According to deficiency of AS in comparison with other relative optimization techniques, some efforts have been done to improve this algorithm.

3.2.2. Elitist Ant System (EAS)

As discussed, much research has been performed to improve the initial version of the ant colony optimization of Section 3.2.1. One of the first improvements that can be enumerated is the Elitist Ant System (EAS) [37]. The main change is based on the idea of increasing pheromone value to the search graph belonging to the best tour found since the start of the algorithm. For adding this additional deposit to the best-so-far tour, the pheromone trail value by the ant with the best tour is also considered.

In order to update the pheromone, an additional value of e/ L_{bs} is added to the search graph, where e is a parameter that defines the weight given to the best-so-far tour, and L_{bs} is the value of objective function corresponding to the best-so-far tour [38]. Therefore, the pheromone update is performed by:

$$\tau_{i,j} = (1-\rho)\tau_{i,j} + \rho\Delta\tau_{i,j} + \varepsilon\Delta\tau_{i,j}^{bs} \tag{3-8}$$

where $\Delta\tau_{i,j}^{bs}$ is defined as follows:

$$\Delta\tau_{i,j}^{bs} = \begin{cases} 1/L_{bs} & , \quad if\ ant\ i,j \in T_{bs} \\ 0, & otherwise. \end{cases} \tag{3-9}$$

Furthermore, pheromone evaporation in EAS is exactly the same as in AS optimization. Comparing AS and EAS shows that utilization of Elitist algorithm may lead to a better solution in less iterations if a proper value of parameter e is applied [37, 38].

3.2.3. Rank-based Ant System (ASrank)

Another improved version of the AS is the rank-based ant system (ASrank). In this algorithm, amount of deposited pheromones is directly related to the ants' rank which is decreased accordingly. Moreover, the best–so-far ants are always recognized with the largest amount of pheromones deposited in each iteration as in the EAS optimization.

The updating process of pheromones is started by sorting the ants based on decreasing their related calculated objective function values. The amount of pheromone is also weighted based on the sorted ants.

Update of Pheromone: Before updating the pheromone trails, the ants are sorted by decreasing their corresponding objective function value and the quantity of pheromone an ant deposits is weighted according to the rank r of the ant. In this process, the best-so-far ants and the number of w-1 ranked ants are able to deposit pheromones. The pheromone update rule of this algorithm can be demonstrated by:

$$\tau_{i,j} = \tau_{i,j} + \sum_{k=1}^{w-1}(w-r)\Delta\tau_{i,j} + w\Delta\tau_{i.j}^{bs} \tag{3-10}$$

where $\Delta\tau_{i.j}^{bs}=1/lbs$, $\Delta\tau_{i,j}^{k} = 1/lk$ (3-11)

L_k is the value of the objective function related to the tour built with ant k and Lbs is the value of objective function corresponding to the best-so-far tour**.** In this case, the strongest feedback is related to the best-so-far tour which has its own weight (w). According to the above rule, the k^{th} is the best ant of the current iteration.

3.2.4. Max-Min Ant System (MMAS)

This algorithm is developed with some modifications on the original Ant System where only the only the best ants can update the pheromones [38].

The best ant is defined as either the ants with the best solution in the current iteration or best- so- far ants which represent the best obtained tour so far. According to abovementioned, all ants might follow the same rules which may affect the population diversity of the program. For this reason, another modification is considered in MMAS where the value of pheromone is bounded.

The pheromone update is implemented as follows:

$$\tau_{i,j} = (1-\rho)\tau_{i,j} + \tau[\Delta\tau_{i,j}^{best}]_{\tau min}^{\tau max} \quad (3\text{-}12)$$

where τ_{max} and τ_{min} are the upper and lower bounds imposed on the pheromone; respectively. The operator $[x]_b^a$ is defined as:

$$[x]_b^a = \begin{cases} a \ \ if \ \ x > a, \\ b \ \ if \ \ x < a, \\ x \quad otherwise; \end{cases} \quad (3\text{-}13a)$$

and

$$\Delta\tau_{i,j}^{best} = \begin{cases} 1/L_{best} \\ 0 \end{cases} \quad (3\text{-}13b)$$

where L_{best} is the length of the tour of the best ant.

Another change in MMAS is the initialization of the pheromone trail to the upper bound which may increase the total amount of the initial pheromone by assuming a little decrease from evaporation of the deposited pheromone. Another modification that has been applied in the re-initialization of pheromone trails when no

improvement has been obtained after certain number of iterations. In regards to the limits, some guidelines have been provided for defining τ_{min} and τ_{max} on the basis of analytical considerations [37, 38].

It is argued that, in MMAS optimization choosing the iteration-best and the best-so-far update rules may cause a great influence on the performance of the algorithm and also on the final solution. In case of performing pheromone update based upon the best- so- far ant, search focuses around the best-tour so-far and for the iteration-best ant, then the number paths which received pheromones is larger and the search is less directed. Therefore, for small optimization problem, best possible solutions can be achieved by using best-so-far ants in the current iteration while for larger problem best-so-far tour is likely to be used [38].

3.3. The Proposed ACAs for Load Interval Division and Optimal Dispatch of LTC and Shunt Capacitors

The application of ACO has been increased in recent years. Generally, different discrete optimization problems are considered to be successfully solved by application of this optimization. ACO algorithms are not only useful for quickly finding high-quality solutions, but also popular for telecommunication network problems. The successful applications of this optimization technique lead to more popularity and tendency to adopt ACO for industrial problems, power system, etc. in order to show its performance in real-world applications.

This research applies ACO to effectively solve the dispatch problem in the present of harmonics caused by nonlinear loads. In addition to its general features, ACO is expected to require less number of iterations to capture a near-optimal solution as compared with other evolutionary based approaches such as GA of Chapter 4. In this optimization technique, load intervals are assigned precisely and optimal solution for the objective function is achieved by simultaneously considering switching and system constraints.

In this regard, two ACO-based algorithms are developed and tested for the determination of optimal load curve interval and the optimal dispatch schedule problem as discussed in the remaining sections of this chapter.

3.3.1. The proposed ACA for Load Interval Division

In this section, the typical daily load curve of Fig. 3.4, the number of intervals is initially assumed and a proposed ACA is utilized to determine the optimal intervals. In order to determine the intervals for the entire load curve (Fig. 3.4) of this optimization that result in a near-optimal LTC schedule (same as GA technique) the number of interval is initially assumed and ACO is utilized to determine the optimal intervals. The LTC tap position remains constant during a load interval and may differ at the next load interval. By having the accurate result of load forecasting, the LTC dispatch obtained in this way can be practically implemented.

The number of interval is assumed to be the number of stages over the length of the entire interval, which is 24 hours. A probability transition rule and roulette method is implemented to find the next tap position. A local pheromone update is important at this stage of optimization in order to avoid identical interval duration. This study considers four intervals and uses the following fitness function [30] to evaluate the possible solutions:

$$F = F_{\max} - \min \sum_{l=1}^{L} \sum_{t=1}^{T} \left[\left(P_{tl} - PA_l \right)^2 + \left(Q_{tl} - QA_l \right)^2 \right] \tag{3-14a}$$

subject to

$$\sum_{l=1}^{L} T = 24 \tag{3-14b}$$

where, F_{max} is the constant that converts fitness function to the standard form, P_{tl} and Q_{tl} are active and reactive powers (at hour t and load interval l), respectively. P_{Al} and Q_{Al} are average active and reactive powers (at load interval l), respectively, T is number of hours at l th load interval and L is the number of assumed interval.

Figure 3.5 shows the flow chart of the proposed ACA for optimal load interval division.

For the process of load interval division by ACO, the flowchart of Fig. 3.5 is applied.

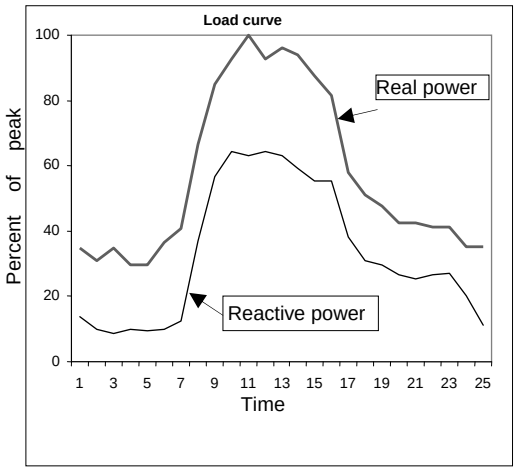

Fig. 3.4. A typical daily load curve [10]

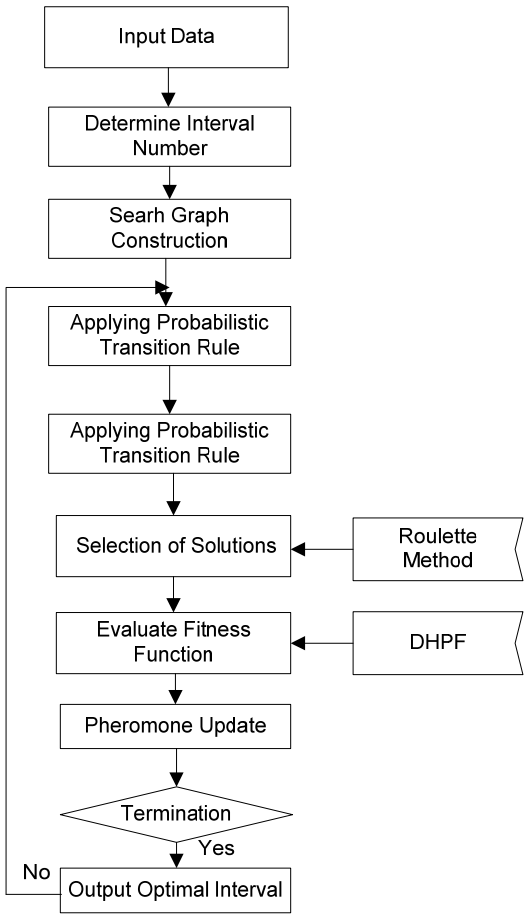

Fig. 3.5. Flowchart of the proposed ACA to determine the optimal load interval division of the daily load curve

3.3.2. The Proposed ACA for Optimal Scheduling of LTC and Shunt Capacitors in the Presence of Harmonics

The proposed ACA for the optimal dispatch problem is based on the initial Ant System considering local update rule similar to the improved Elitist algorithm. Optimization is performed by a cycle of five stages: initialization, graph construction, probabilistic transition rule, local updating, objective function, and global updating:

(A) Initialization

As per all ACO algorithms, initial values of the pheromone and parameter are important and will be defined for the proposed algorithm. A power flow algorithm (or a harmonic power flow algorithm as discussed in Chapter 2) is required for initialization of the pheromone trail in order to calculate the maximum value of the objective function. In order to find the optimal interval of the load curve and the optimal solution of the dispatch, the number of ants and required parameters (α, β and φ) are initially constituted. Parameter values and the number of ants may vary in different optimization problems.

(B) Construction Graph

It is essential to construct a predefined graph to demonstrate the possible tour as shown in Fig 3-6 [37]. This search graph demonstrates the entire setting of the control parameters of the problem in which the ants walk and create their tours. For this optimization problem, control parameters are assumed to be LTC ratios, reactive power of the shunt capacitors and all possible switching settings. These control settings perform number of stages of the aforementioned search graph [38].

In other words, the number of stages is equal to the number of control parameters of the optimization problem and the number of states of each stage is equal to the number of possible solutions for the related control parameter. Therefore, the number of states is not necessarily the same in all stages.

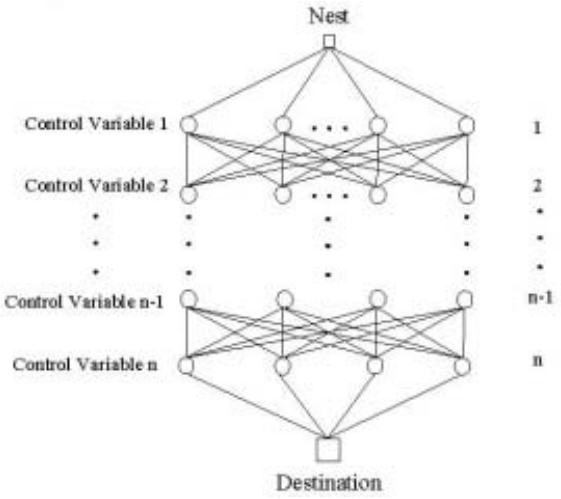

Fig. 3.6. Search Graph for Optimization Problem [38]

(C) Probabilistic Transition Rule

As shown in ACO algorithm (Fig. 3.5), each ant starts the search process by choosing the next state according to the probabilistic transition rule based on Eq. (3-2).Therefore, the tour will proceed by moving from one stage to another stage and updating the list of possible paths visited by ants. For each probability, a roulette method is implemented to select ants for the next path. In this method, first the selection probability of each path is distributed based on the pheromone values for a path [31] and then a random number is produced. The selected path and its corresponding information are defined according to the random number calculated by the roulette wheel.

(D) Local Update Rule

For the proposed ACO procedure, a local pheromone update needs to be considered at the end of the construction process. Upon the completion of each tour, each ant updates the local pheromone as shown in Eq. (3-4).

(E) Objective Function

The objective function of the scheduling problem is minimization of energy loss over a 24-hour period:

$$min \sum_{t=1}^{24} P_{loss}(Q_t, T_t) * \Delta t \tag{3-15}$$

where P_{loss} is total power loss at hour t as a function of Q_t and T_t that are the statuses of shunt capacitors and LTC tap position, respectively. While, Δt is time interval that

is normally taken as 1 hour. This objective function is subjected to the following constraints:

- Voltage constraint

$$V_{i\,min} \le V_{irms} \le V_{i\,max} \tag{3-16}$$

where $V_{i\ min}$ and $V_{i\ max}$ are the respective minimum and maximum limits of *rms* voltage at bus *i* (V_{irms}).

- Total harmonic distortion of voltage (THD_v)

$$THD_{vi} \le THD_v^{max} \tag{3-17}$$

where THD_{vi} and THD_v^{max} are the distortion at bus *i* and the maximum distortion allowed, respectively.

- Maximum switching operation of LTC

$$\sum_{t=1}^{24} \left| TAP_t - TAP_{t-1} \right| \le K_T \tag{3-18}$$

where TAP_t and K_T are LTC tap position at hour *t* and maximum LTC switching, respectively.

- Maximum switching operation of shunt capacitors

$$\sum_{t=1}^{24} \left(C_{nt} \oplus C_{nt-1} \right) \le K_c; \quad n = 1, 2, ..., nc \tag{3-19}$$

where C_{nt} and C_{nt-1} are the status of capacitor *n* at hours *t* and *t*-1, respectively. $\oplus$ represents the logic operator XOR (exclusive or) that returns "1" if $C_{nt} \ne C_{nt-1}$ and returns 0 if $C_{nt} = C_{nt-1}$. While K_c and *nc* are the maximum limit of capacitor switching and the number of shunt capacitors, respectively.

Evaluation of the best fitness is performed by simultaneously considering the objective function and constraints.

(E) Global Updating Process

The global update is performed at the end of each cycle when solutions are evaluated. At this step, pheromone trails are updated based on the best solution

taking into consideration the evaporation and deposition of pheromone. Evaporation decreases the level of pheromone by Eq. (3-5).

The pheromone evaporation is important to be considered as it avoids increasing the level of pheromones and helps the mechanism to forget bad decision of the past. After evaporation, all ants lay down pheromone on the paths based on Eq. (3-6).

Therefore, the global updating rule will increase the capability of the procedure in finding the optimal solution. The above-mentioned five-step cycle is repeated at each iteration. After either a predefined number of iterations, or the algorithm converges and the best solution represents a near-optimal solution

Figure 3.7 shows the flow chart of the proposed ACA for optimal dispatch of LTC and switched shunt capacitors in the presence of harmonics.

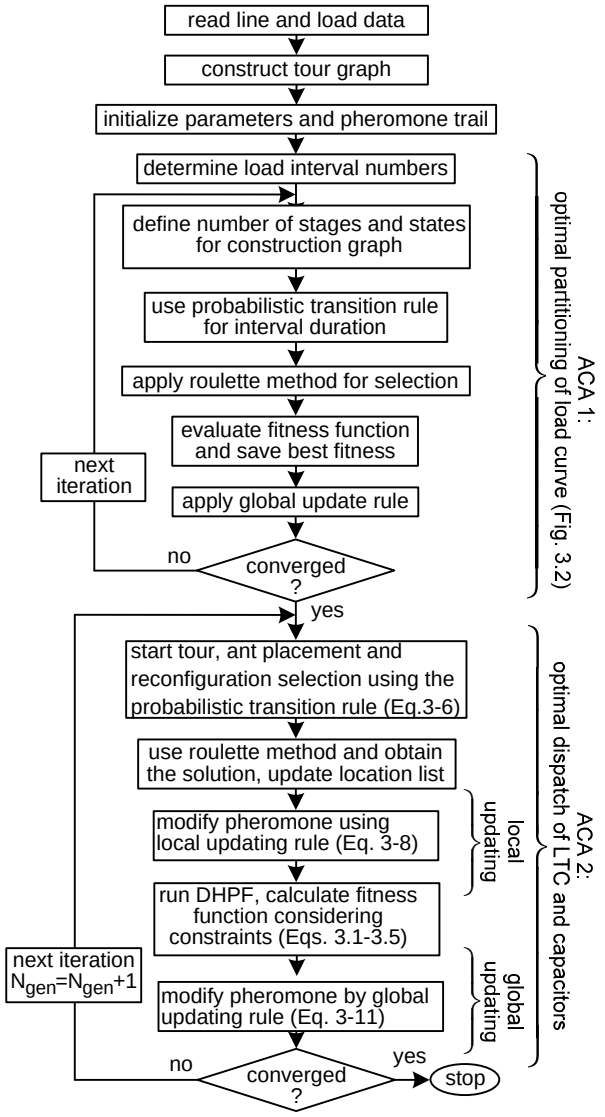

Fig. 3.7. The proposed ACA for optimal scheduling of LTC and shunt capacitors for sinusoidal and non-sinusoidal operating conditions.

CHAPTER FOUR

APPLICATION OF GENETIC ALGORITHMS FOR OPTIMAL DISPATCH OF LTC AND SWITCHED SHUNT CAPACITORS

This chapter presents the application of genetic algorithm (GA) for scheduling load tap changers and shunt capacitors under non-sinusoidal operating conditions based on the genetic proposed in reference [1]. This intelligent genetic approach will be used in Chapter 5 to evaluate the performance, accuracy and convergence of the proposed ACA of Chapter 3.

4.1. Genetic Algorithm

Genetic Algorithm is considered as one of the most powerful approaches in capturing the near global optimal solution of nonlinear problems [43-45]. It performs very well on mixed (continuous and discrete) and combinatorial nonlinear problems. GA follows the principle of natural evolution to obtain the optimal solution. Coding and encoding capability of this technique may lead to a better solution as compared to other optimization methods.

On the other hand, as the optimization is based upon random selection of population, the process is usually slow and requires more iterations to converge to a near-global solution. For the dispatch problem with nonlinear loads on the distribution system, multiple executions of the harmonic power flow algorithm are usually performed at each iteration that will further increase the required computing time.

4.1.1. The GA Optimization Procedure

In a genetic optimization algorithm, an initial population of individuals (strings) is firstly constructed to evolve toward better solutions. These initial individuals are assumed as the data structure which is used in the optimization process. Traditionally, the evolution starts with generating random individuals. In each generation, individuals are evaluated with respect to their fitness. In order to form new population, individuals are modified in terms of recombination and mutation of individuals. This transformation is performed in two stages. New individuals are created by small changes in one individual or by combining parts of different

individuals. The new population is then used in the next iteration of the algorithm. Generally, the algorithm terminates when either no improvement is obtained or a maximum number of generations has been produced. If the algorithm is terminated due to a maximum number of generations, a satisfactory solution (near-optimal solution) may or may not have been reached. The description of the GA procedure is considered as follows [46-51]:

(A) Initialization

For the initialization, chromosomes are randomly generated to form an initial population. The population size depends on the nature of the problem, but typically contains several hundreds or thousands of possible solutions. These initial chromosomes are made of binary strings which consist of substring and represent a potential solution of the optimization problem.

(B) Fitness Evaluation

A fitness function is defined to evaluate the solution domain. This function links the problem to the algorithm. Fitness depends on the predefined objective function of the optimization problem. The fitness of the solution has a great impact on the optimal solution and needs to be considered precisely. In this process, fitness function is measured for each chromosome and the best solution is obtained based on the fittest chromosome. Accordingly, all individuals are selected and classified. The fitter chromosomes might have more chance to be utilized in the GA process.

After defining the fitness function, GA starts to randomly initialize a population, and then improves it through repetitive application of mutation, crossover, inversion and selection operators.

(C) Selection

Selection is the first step after evaluating all individuals. There are various selections methods to rate the fitness of each solution. The most popular and well-studied techniques in this regard are *Roulette Wheel* and *Tournament Selection*. In order to perform the selection based on the *Roulette Wheel* method, a circle with slots sized based on fitness of chromosomes is constructed. The chromosomes are then selected according to the spin of roulette wheel to form a new population [46]. Tournament

selection is considered as ranking chromosomes based on their fitness value. The best solution is selected in one generation to form a new population. This process is repeated until the new population is generated. Number of chromosomes depends on the size of tournament defined in the algorithm. In this method, chromosomes are randomly selected. The outcome of selection process is the establishment of a new population in which the chromosomes are likely to be similar. This is due to evaluation of the chromosomes based on fitness value.

(D) Crossover

Crossover is defined as generating a second-generation population of solutions. A new population is created by exchanging segments between two possible solutions. In other words, two existing chromosomes (parents) are selected to produce the new solution (child). The new solution obtains many of the characteristics of its parents.

(E) Mutation

Mutation process is selected as one of the important genetic operators in GA optimization. Mutation is random modification of the genes in the population considering a predefined probability. This is implemented by changing the bits from 1 to 0 or vice-versa which gives more variability into the population. This will cause extra searching throughout the process in order to prevent local optimal solution.

(F) Termination

After completion of the abovementioned process, the new generation needs to be evaluated. The generation process is repeated until a termination condition is achieved.

4.1.2. Constraint

In optimization problems, the number of constraints might be considered depending on what objective function is defined or which system is under study. Constraints are usually assigned by assuming their formulations in the optimization calculations. In regards to the constraints, the consequence of their violation on fitness value is evaluated. This violation may be assumed as penalties into the system. By imposing penalties, the violation of the constraints will be considered in the optimization process.

4.1.3. Elitism

Elitism is the process of selecting the better individuals, or in other words, selecting individual with a bias towards the better one. Elitism is important since it allows the solution to get better over time. If only the few best parents are picked and the worst are replaced, then the solution might not be sub-optimal [44, 45]. In Elitism, best individuals who are preserved from the last generation will be directed to the next generation. In this process, the best solution will be kept and transferred to the next iteration without being modified through crossover or mutation stages. The best population will then be evaluated against the new best solution of each generation.

4.2 Application of GA in Optimal Dispatch of LTC and Shunt Capacitors

Reference [1] proposes a GA approach for the optimal dispatch of LTC and switch capacitor banks for non-sinusoidal operating conditions. It presents detailed analysis, formulation and simulation results that will not be repeated here since the main objective of this thesis is to develop a new dispatch approach based on AC optimization as presented in Chapter 3.

Figure 4.1 shows the flow chart of the dispatch GA of [1]. This algorithm has been coded in MATLAB (version 7.0.1) and will be used in Chapter 5 to evaluate the performance of the proposed ACA.

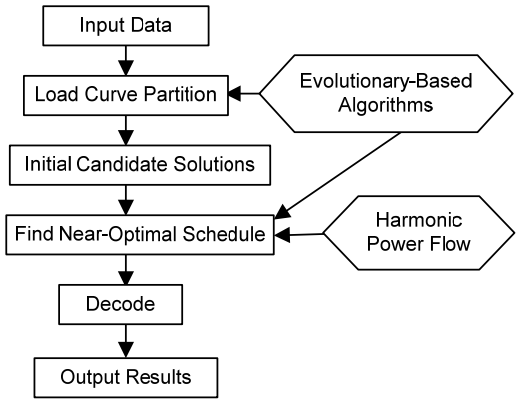

Fig. 4.1. Flowchart of GA for optimal scheduling of LTC and shunt capacitors considering harmonic distortions [1]

CHAPTER FIVE

SIMULATION RESULTS FOR OPTIMAL DISPATCH OF LTC AND SHUNT CAPACITORS CONSIDERING HARMONIC DISTORTIONS

This chapter provides detailed simulation results to evaluate the performance of the proposed ACA for the optimal dispatch of LTC and switched shunt capacitors under non-sinusoidal operating conditions. Detailed simulations are performed, compared and analysed based on the proposed ACA [51] and the introduced GA [1] of Chapters 3 and 4, respectively. Some results are also compared with a GA-Fuzzy optimization approach that has been recently proposed in the literature [2]. The impacts of voltage and current harmonics on the optimal scheduling are deeply studied in terms of variations in voltage profile, increased in total power loss and THD distortion. The developed optimization techniques are implemented for the IEEE 31-bus and 123-bus distorted distribution systems.

5.1. GA-Based Evolutionary

Two GAs are utilized; one for optimal load division and the other for the optimal scheduling of LTC and switched shunt capacitors. GA is started by the initialization process which consists of randomly generating the initial chromosomes and loading input data. For the objective function of the optimization problem, switching constraints are important to be satisfied. Therefore, only initial chromosomes that satisfy the switching constraints are selected to construct the initial population. In the next step, parents are created by applying the tournament method [46]. Modified chromosomes are generated as children based on the one-point crossover procedure [52]. It is assumed that the probability of crossover and mutation, population size, and weighting coefficients are fixed throughout the generation. In each generation, the proper solutions created by evaluating the fitness function is computed and saved to be used in the following generation by applying Elitism scenario. This optimization technique is discussed in Chapter 4. Fitness function and problem constraints are utilized for the scheduling problem as presented in Chapter 3.

In regards to GA optimization in this research, the initial number of chromosomes and the maximum number of iterations are assumed to be 30 and 50, respectively. In

addition, the tournament size is assumed to be 3 chromosomes and the crossover and mutation rates are set to 60% and 1%, respectively. Convergence is an important issue. The genetic algorithm tries to avoid premature convergence by monitoring the evolution of generations. This is achieved by employing a procedure to discover the possible premature convergence. According to this procedure, number of generations will no longer increase if no progress is achieved in terms of fitness improvement after three frequent generations. This leads to less computation time in case of having no progress. To sum up, the algorithm terminates when it reaches the maximum number of generation or no improvement is achieved in terms of the fitness function.

5.2. ACO-Based Evolutionary

The AC based algorithm of Chapter 3 is developed and simulated for optimal dispatch of LTC and shunt capacitors. As with the genetic algorithm, two optimization algorithms are utilized. In order to obtain optimal dispatch of LTC and shunt capacitors over 24 hours, an optimal load interval is required in advance. Therefore, the proposed AC algorithm is applied twice with the same concept and formulations using slightly different parameters. In implementing the AC algorithm for the IEEE 31-bus system, a total number of 11 stages including 2 shunt capacitors on the substation and 5 shunt capacitors on the feeder are selected. Transformer tap ratios will remain constant during each interval and therefore, 4 states (corresponding to the assumed 4 total intervals) are considered in this optimization problem. In regards to the switching of shunt capacitors, numbers of states are equal to 2 steps according to the switching status over 24 hours.

The AC algorithm is developed in MATLAB (version 7.0.1) with the following parameters: α =1, β=1 and ρ=0.5. The initial value of the pheromone is assumed to be 0.75. As discussed in Chapter 3, parameter f represents the estimated maximum value of objective function. For calculating f, a power flow (or a harmonic power flow) algorithm is required for sinusoidal (or non- sinusoidal) operating condition. According to the selected number of load intervals (equal to 4 in this research) and the system data, simulations are performed for 14 ants and the maximum number of generation is set to 50.

5.3. Optimal Scheduling of the IEEE 31-Bus System

The developed ACA and GA are employed for the 31-bus distribution system (Fig. 5.1) to obtain the optimal scheduling of LTC and shunt capacitors. Generally, the presentation of this chapter begins with a small system and continues with more complicated cases. The simulation results compare the efficiency and accuracy of these two powerful AC and genetic techniques. The simulations are performed for non-sinusoidal operating condition by considering multiple nonlinear loads in the distribution system.

5.3.1. System Data

The IEEE 31-bus system from [10] including multiple nonlinear loads is considered in this section as shown in Fig 5.1. The data of nonlinear loads are given in Tables 5.2 and 5.6, and their harmonic spectrums and waveforms are given in Table 5.6. The simulation results demonstrate the application of the GA and ACA optimization for the given system. The objective function of this scheduling problem is presented in Chapter 3 Eq. (3-15) which is based on power loss minimization over the 24 hours period. The optimization constraints are set based on Eqs. (3.16-3.19) of Chapter 3.

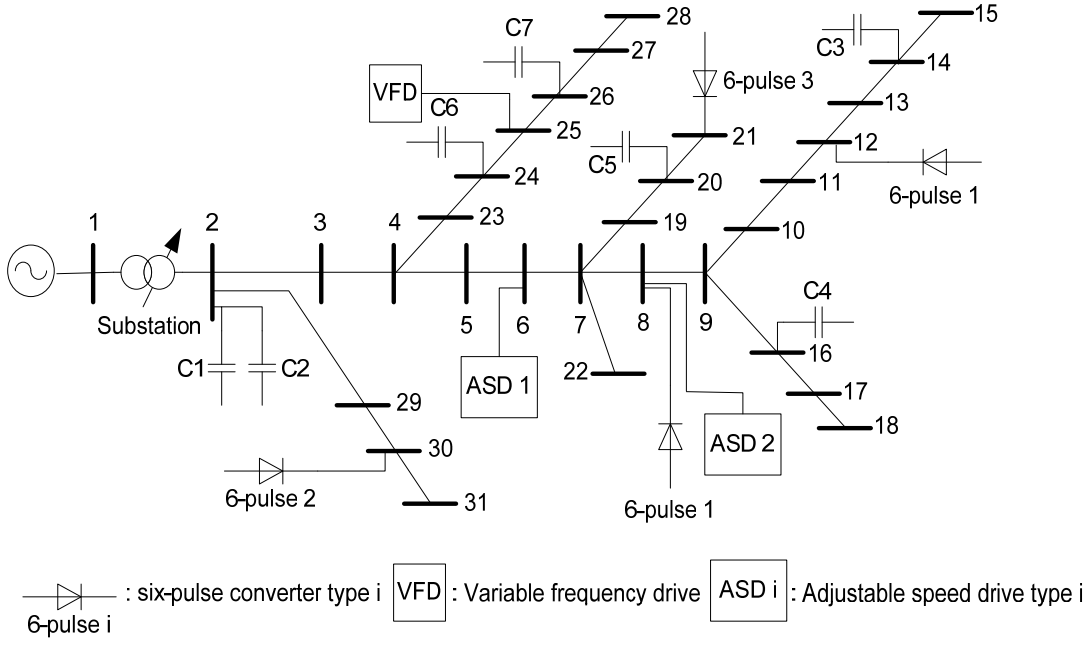

Fig. 5.1.The highly distorted 31-bus system with multiple nonlinear loads used for simulations

Table 5.1
Capacitor Data for Distribution System [10]

Capacitor	C1	C2	C3	C4	C5	C6	C7
Bus Location	2	2	14	16	20	24	26
Size (kVAr)	900	600	600	600	300	900	900

Table 5.2a
Nonlinear load data for 31-bus distribution system (Fig. 5.1)

Nonlinear Bus	Nonlinear Load Type	kW	kVAr
6	PWM adjustable-speed drive, type 2 (ASD 2)*	575	326
8	six-pulse, type 1 (6-pulse 1)**	436	231
8	PWM adjustable-speed drive type 1 (ASD 1)*	247	158
12	six-pulse, type 1 (6-pulse 1)**	347	176
21	six-pulse, type 3 (6-pulse 3)**	315	156
25	six-pulse variable-frequency drive (VFD)	454	229
30	six-pulse, type 2 (6-pulse 2)**	527	242

*) Two types of typical PWM drives are selected.

**) Three types of typical six-pulse loads are selected.

5.3.2. Simulation Results Based on AC and GA

The near-optimal dispatch of LTC and shunt capacitors for the IEEE 31-bus system considering harmonics is generated using ACA and GA. Simulation results are shown in Tables 5.3 and 5.4 and Figs. 5.2-5.4. The original tap position of LTC is 0 and the initial status of all capacitors is "off" (0). Multiple nonlinear load currents are injected to the system which makes the calculations complicated. The fulfilment of switching constraints is checked and it is confirmed that the constraints are fully satisfied.

Fig. 5.3 shows the voltage improvement using both algorithms. For this IEEE 31-bus system, GA results for voltage improvement are slightly better for ACA. However, the voltage deviations of both approaches are within the designated 10% limit. According to Fig. 5.2 and Fig. 5.4, both methods have successfully reduced the hourly power losses and maintained the acceptable THD_V levels. The summary of optimization results are given in Table 5.4.

Table 5.3
The optimal dispatch schedules of LTC and shunt capacitors of 31-bus system (Fig. 5.1) for non-sinusoidal operating condition using GA and ACA

Hour	GA								ACA							
	LTC	C1	C2	C3	C4	C4	C6	C7	LTC	C1	C2	C3	C4	C4	C6	C7
1	3	0	0	0	0	0	0	0	5	0	0	0	0	1	1	0
2	3	0	0	0	0	0	0	0	5	0	0	0	0	1	1	1
3	3	0	0	0	1	0	0	0	5	0	0	0	0	1	1	0
4	3	0	1	0	1	1	0	0	5	0	0	0	0	1	1	0
5	3	0	1	0	1	1	1	0	5	0	1	0	0	1	1	0
6	3	0	1	0	1	1	1	0	5	1	1	0	0	1	1	0
7	3	0	0	0	1	1	1	0	5	0	0	0	0	1	1	0
8	3	0	0	1	1	1	1	0	5	0	0	0	0	1	1	0
9	3	1	1	1	1	1	1	0	5	1	0	0	1	0	1	0
10	4	1	1	1	1	1	1	1	-2	1	0	0	1	0	1	0
11	4	1	1	1	1	1	1	1	-2	1	0	0	1	0	1	0
12	4	1	1	1	1	1	1	1	-2	1	1	1	1	0	1	0
13	4	1	1	1	1	1	1	1	-2	0	1	1	1	0	1	0
14	4	1	1	1	1	1	1	1	6	0	1	1	1	0	1	0
15	4	0	0	1	1	1	1	1	6	0	0	1	1	0	1	0
16	4	0	0	1	1	1	1	1	-3	0	0	1	1	0	1	0
17	3	0	0	1	1	1	1	0	-3	1	0	1	1	0	1	0
18	3	0	0	1	1	1	1	0	-3	0	0	1	1	0	1	0
19	3	0	0	1	0	1	1	0	-3	0	1	1	1	0	1	0
20	3	0	0	1	0	1	1	0	-3	0	1	1	0	0	1	0
21	3	0	0	1	0	1	1	0	-3	0	0	0	0	0	1	0
22	3	1	0	1	0	1	1	0	-3	0	0	0	0	0	1	0
23	3	1	1	0	0	1	1	0	-3	0	0	0	0	0	1	0
24	3	0	0	0	0	0	0	0	-3	0	0	0	0	0	1	0

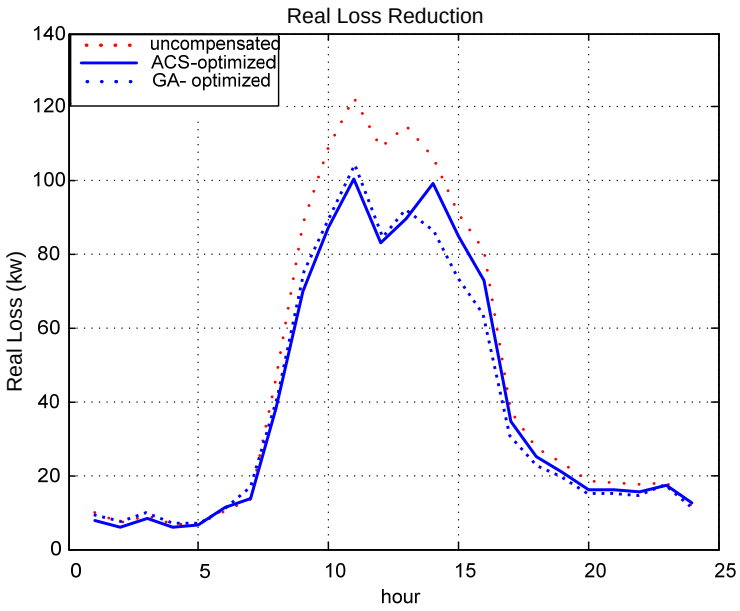

Fig. 5.2. Hourly reduction of real power loss for the 31-bus system (Fig. 5.1) under non-sinusoidal operating condition using GA and ACA

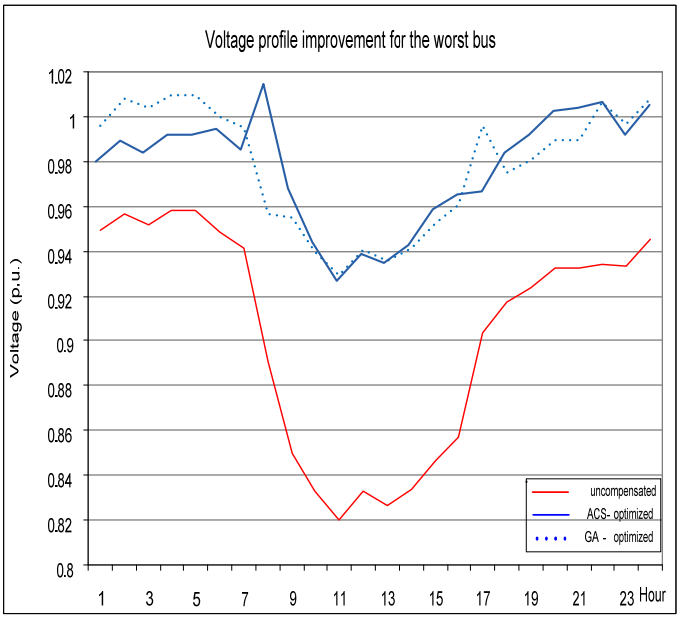

Fig.5.3. Voltage improvement of the worst bus (Fig. 5.1, bus 15) under non-sinusoidal operating condition with multiple nonlinear loads

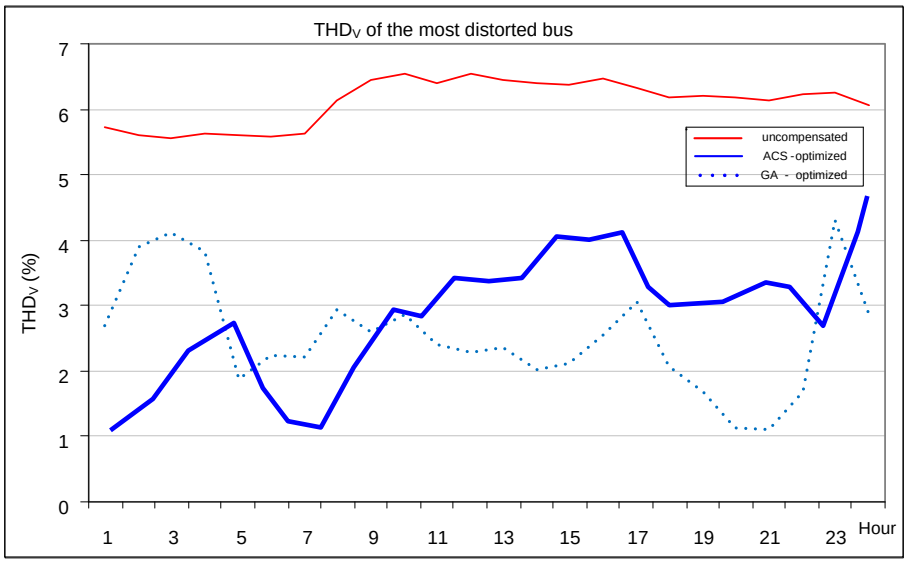

Fig. 5.4. THD_V reduction of the most distorted bus (Fig.5.8, bus 26) for 31-bus system using GA and ACA

Table 5.4
Optimization benefits of 31-bus system including multiple nonlinear loads under non-sinusoidal operating condition using GA and ACA

Optimization Benefits	GA	ACA
Energy Saving (MWh)	278.16	267.87
Average Voltage Improvement (%)	7.49	7.46
Average THD reduction (%)	3.20	3.04
Computation time (sec)	2063.92	1028.02

5.4. Optimal Scheduling for IEEE 123-bus System

As realistic distribution systems usually consist of a large number of buses and nonlinear loads, the performance and abilities of the optimal scheduling of LTC and shunt capacitors needs to be investigated for large distributions systems. In this view, the IEEE 123-bus system of Fig. 5.5 [1, 53] with 14 shunt capacitor banks and 12 nonlinear loads is simulated in this section. In this study, both the ACA of Chapter 3 and the GA of Chapter 4 [1] are utilized for the optimal scheduling problem. For further evaluation of the proposed ACA, simulation results are also compared with the recently proposed GA-Fuzzy dispatch approach of [2]. All optimizations are carried out considering multiple nonlinear loading and the presence of current and voltage harmonics. The significance of including harmonics is emphasised and highlighted.

5.4.1. System Data

The IEEE 123-bus system [1] with the addition of 14 shunt capacitor banks (Table 5.5) and 12 nonlinear loads (Tables 5.7) is used in this section. Nonlinear loads are modelled with harmonic current sources (Table 5.6) and linear loads are presented as 50% constant impedance and 50% constant power. The peak of both real and reactive loads are assumed to change according to Fig. 3.4 of Chapter 3. The maximum and minimum voltage limits at every bus are 1.05 pu and 0.95 pu, respectively. The allowable maximum switching operation of LTC is 30, while the maximum switching allowed for shunt capacitors on the substation and on the feeder are 6 and 2, respectively. The original tap position of LTC is 0 and the initial status of all capacitors is "off" (0). Simulations are performed and compared using ACA, GA, and GA-Fuzzy.

Table 5.5
The shunt capacitor data for the IEEE 123-bus system (Fig. 5.5) from [1]

Shunt Capacitor	Location	kVAr
C1	1	50
C2	1	50
C3	13	50
C4	18	50
C5	35	50
C6	44	100
C7	57	50
C8	60	100
C9	72	50
C10	81	100
C11	86	50
C12	101	50
C13	110	100
C14	114	100

Table 5.6
Harmonic spectrums of nonlinear loads (Fig. 5.1, Table 5.2) from [2]

order	six-pulse, **type 1**		six-pulse, **type 2**		six-pulse, **type 3**	
	magnitude (%)	phase (^{o})	magnitude (%)	phase (^{o})	magnitude (%)	phase (^{o})
1	100	0	100	0	100	0
5	20	0	19.1	0	42	0
7	14.3	0	13.1	0	14.3	0
11	9.1	0	7.2	0	7.9	0
13	7.7	0	5.6	0	3.2	0
17	5.9	0	3.3	0	3.7	0
19	5.3	0	2.4	0	2.3	0
23	4.3	0	1.2	0	2.3	0
25	4	0	0.8	0	1.4	0
29	3.4	0	0.2	0	0	0
31	3.2	0	0.2	0	0	0
35	2.8	0	0.4	0	0	0
37	2.7	0	0.5	0	0	0
41	2.4	0	0.5	0	0	0
43	2.3	0	0.5	0	0	0
47	2.1	0	0.4	0	0	0
49	2	0	0.4	0	0	0

order	variable-frequency drive*		adjustable-speed drive*	
	magnitude (%)	phase (^{o})	magnitude (%)	phase (^{o})
1	100	0	100	0
5	23.52	111	23.52	111
7	6.08	109	6.08	109
11	4.57	-158	4.57	-158
13	4.2	-178	4.2	-178
17	1.8	-94	1.8	-94
19	1.37	-92	1.37	-92
23	0.75	-70	0.75	-70
25	0.56	-70	0.56	-70
29	0.49	-20	0.49	-20
31	0.54	7	0.54	7

*) A variable frequency drive (VFD) refers to AC drives only and a variable speed drive (VSD) refers to either AC drives or DC drives.

Table 5.7
Nonlinear load data for the IEEE 123-bus system (Fig. 5.5) from [2]

Nonlinear bus	Nonlinear load type	kW	kVAr
13	six-pulse, type 2 (6-pulse 2)*	24.7	17.6
15	six-pulse, type 1 (6-pulse 1)*	31.5	19.6
21	six-pulse, type 3 (6-pulse 3)*	38.3	26.4
25	six-pulse variable-frequency drive	35.4	17.9
40	PWM adjustable-speed drive	47.4	29.3
54	six-pulse, type 2 (6-pulse 2)*	38.2	15.1
64	six-pulse, type 1 (6-pulse 1)*	21.3	9.3
74	six-pulse, type 3 (6-pulse 3)*	25.7	17.2
78	six-pulse variable-frequency drive	38.4	14.2
100	PWM adjustable-speed drive	24.7	18.4
106	six-pulse, type 1 (6-pulse 1)*	19.2	9.4
610	six-pulse variable-frequency drive	38.5	19.5

*) Three types of typical six-pulse loads are selected.

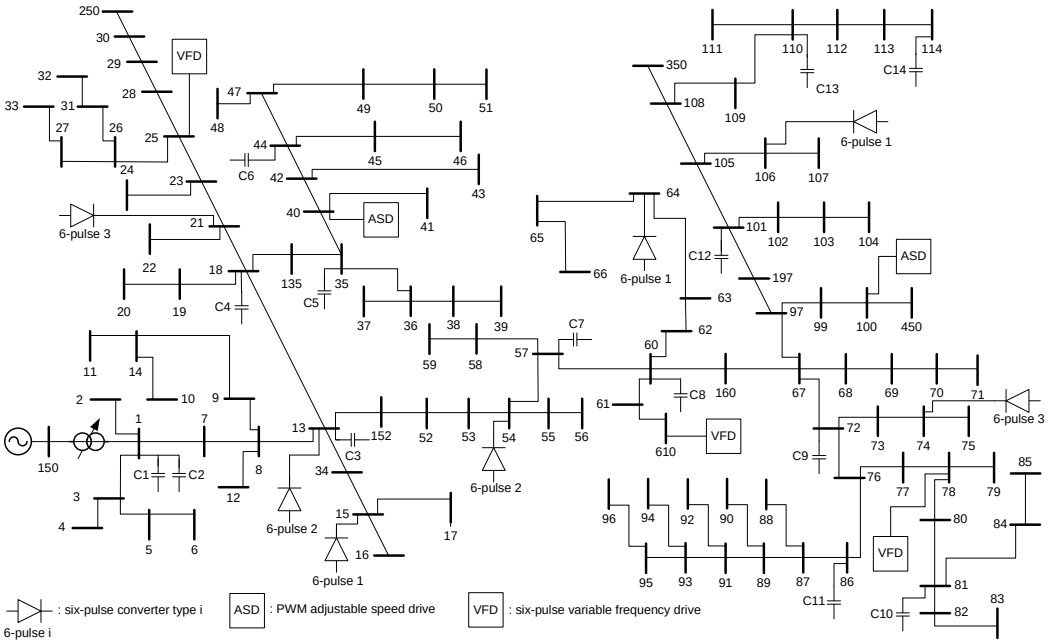

Fig. 5.5. The IEEE 123-bus distorted distribution system including multiple nonlinear loads used for simulations

5.4.2. Formulation of Optimal Dispatch Problem

Dispatch Objective Function:

The objective function of the scheduling problem is the minimization of energy loss over a 24-hour period as outlined in Chapter 3 (Eqs. 3-15).

Optimization Constraints:

The dispatch objective function is subjected to the following constraints which are also discussed in Chapter 4 (Eqs. 4-16-4-19):

- Voltage constraint- The upper and the lower limits of voltage magnitudes at all buses are controlled and limited to the predefined limits of 0.9pu and 1.0pu, respectively. The AC, GA and GA-Fuzzy algorithms perform this action by optimal setting and switching of LTC and shunt capacitors.
- Total harmonic distortion of voltage (THD_v)- The THD of voltages at all buses are controlled and limited to 5% as recommended by the IEEE 519 std [54].
- Maximum switching operation of LTC and shunt capacitors. For realistic considerations of the number of LTC and capacitor switching, upper limits are considered and enforced in the optimization algorithms.

5.4.3. Evolutionary Strategy of Proposed AC Optimization

In implementing the AC algorithm, a total number of 18 stages including 4 levels of LTCs, 2 shunt capacitors at the substation and 12 shunt capacitors at the feeder are considered. Transformer tap ratios will remain constant during each interval and therefore, 4 states (corresponding to four assumed load intervals) are considered. In regards to the switching of shunt capacitors, numbers of states are equal to 2 steps according to the switching status over 24 hours.

The ACA is developed in MATLAB (version 7.0.1). The heuristic information is defined as transformer tap ratios and the reactive power of the shunt capacitors. The selected ACA parameters are: α =1, β=1, ρ=0.5, initial value of pheromone calculated by (Eq. 3-1) is assumed to be 0.75, number of load intervals= 4, number of ants= 14, and maximum number of iteration= 50. For the optimal dispatch problem of this thesis, the best solution is achieved after 35 iterations which is less than the iterations required by GA and GA-Fuzzy as outlined in the next section. As with the

GA, weighting coefficients influence the results and, on the other hand, different runs of the ACA tends to generate slightly different results even for the same initial conditions. Defining the best values for the weighting coefficients, initial population and the maximum number of iterations is expected to generate accurate results with reasonable computation times.

5.4.4. Simulation Results based on AC, GA and GA-Fuzzy

The near-optimal scheduling of LTC and shunt capacitors for the distorted IEEE 123-bus system is performed using ACA, GA [1] and GA-Fuzzy [2]. Simulation results for the operational and switching constraints of Table 5.8 are presented in Tables 5.9-5.10 and Figs. 5.6-5.9. The original tap position of LTC is 0 and the initial status of all capacitors is "off" (0).

Table 5.8
Constraints of optimal dispatching based on ACO, GA and GA-Fuzzy

maximum switching of LTC	30 per day
maximum switching of substation capacitor	6 times per day
maximum switching of feeder capacitor	2 times per day
bus voltage deviation	0.95pu -1.05pu
THD_V limit	5 %

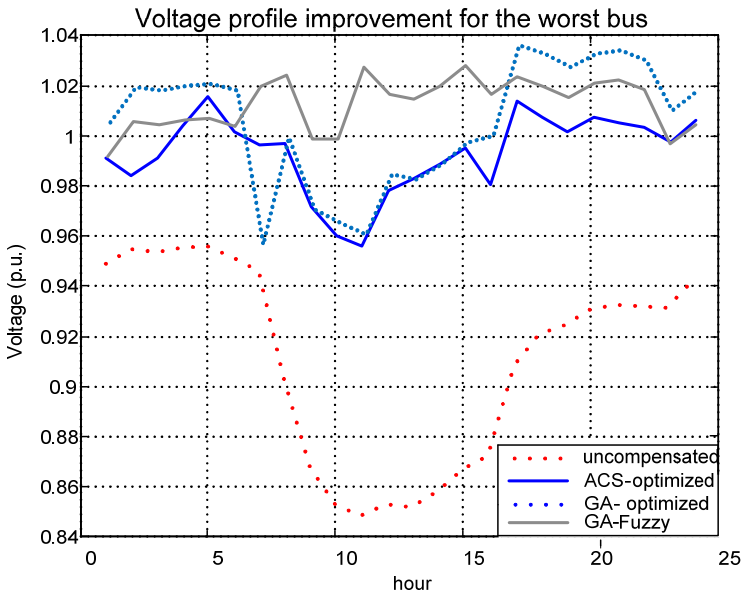

Fig. 5.6. Voltage improvement at the worst bus (Fig. 5.5, bus 114) with GA, GA-Fuzzy and ACA optimizations

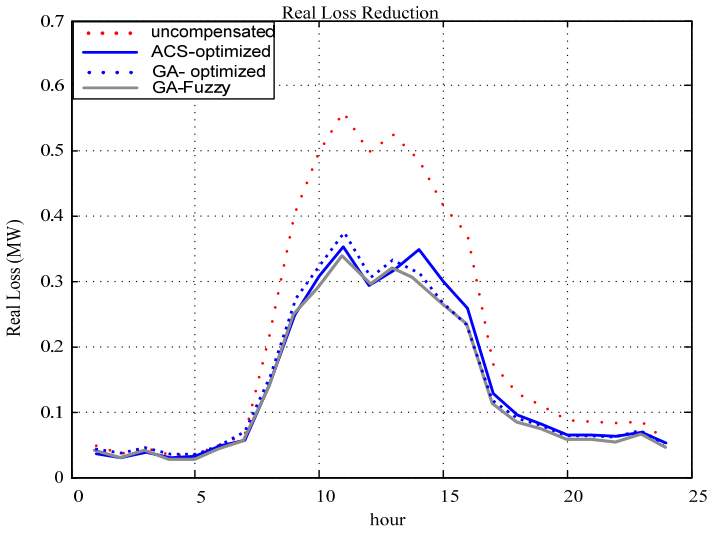

Fig. 5.7 Reduction of real power loss for the IEEE 123-bus system with GA, GA-Fuzzy and ACA optimizations

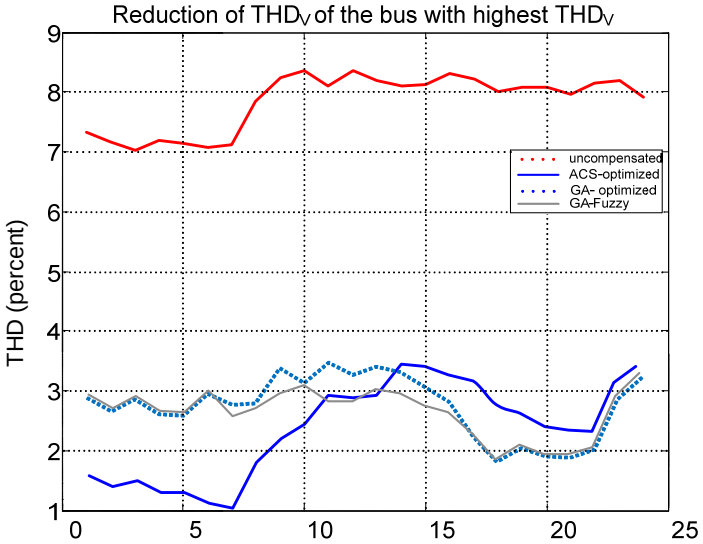

Fig. 5.8. Reduction of THD_V for the IEEE 123-bus system with GA, GA-Fuzzy and ACA optimizations

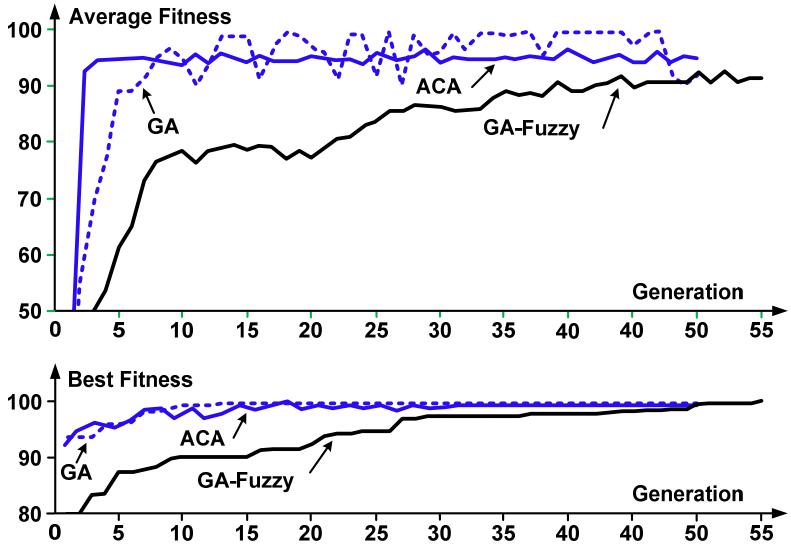

Fig. 5.9. Average and best fitness functions of GA, GA-Fuzzy and ACA optimizations.

Table 5.9
Optimal scheduling of LTC and shunt capacitors for the 123-bus system of Fig. 5.5 with 12 nonlinear loads based on the proposed ACA (Fig. 3.7), GA [1], and GA-Fuzzy [2]

hour	LTC	C1	C2	C3	C4	C5	C6	C7	C8	C9	C10	C11	C12	C13	C14
Optimal scheduling based on the proposed ACA (Fig. 3.7)															
1	7	0	0	0	0	0	1	1	1	0	0	0	0	0	0
2	7	0	0	0	0	0	1	1	1	0	0	0	0	0	0
3	7	0	0	0	0	0	1	1	1	0	0	0	0	0	0
4	7	0	0	0	0	0	1	1	1	1	1	0	0	0	0
5	7	0	0	0	0	0	1	1	1	1	1	0	0	0	0
6	7	0	0	1	1	0	1	1	1	1	0	0	0	0	0
7	7	0	0	1	1	1	1	1	1	0	0	0	0	0	0
8	7	0	0	1	1	1	1	1	1	0	0	1	0	0	0
9	7	0	0	1	1	1	1	1	1	0	0	0	0	0	1
10	7	0	0	1	1	1	1	1	1	0	0	0	0	0	1
11	7	1	0	1	1	1	1	1	1	0	1	0	0	0	1
12	7	1	0	1	0	1	1	1	1	0	1	0	0	1	0
13	7	1	0	1	0	1	1	1	1	0	1	0	0	1	0
14	3	1	0	1	0	0	0	1	1	0	1	0	1	1	0
15	3	0	0	1	0	0	0	1	1	0	1	0	1	1	0
16	3	0	0	1	0	0	0	1	1	0	1	0	1	1	0
17	2	0	1	1	0	0	0	1	1	0	1	0	1	0	0
18	2	1	0	1	0	0	0	1	1	0	1	0	1	0	0
19	2	1	0	1	0	0	0	1	1	0	1	0	1	0	0
20	2	0	1	1	0	0	0	1	1	0	1	0	1	0	0
21	2	0	0	1	0	0	0	1	1	0	1	0	1	0	0
22	2	0	0	1	0	0	0	1	1	0	1	0	1	0	0
23	2	0	1	1	0	0	0	0	0	0	1	0	0	0	0
24	2	0	1	0	0	0	0	0	0	0	0	0	0	0	0
Optimal scheduling based on GA [1]															
1	4	1	0	0	0	1	0	0	0	1	0	0	0	0	0
2	4	1	0	0	0	1	0	0	0	1	1	0	0	0	0
3	4	0	0	0	0	1	0	0	0	1	1	0	0	0	0
4	4	1	0	0	0	1	0	0	0	1	1	0	0	0	0
5	4	1	0	0	0	1	0	0	0	1	1	0	0	0	0
6	4	0	0	1	0	1	0	0	0	1	1	0	0	0	0
7	-1	1	0	1	0	1	0	0	1	1	1	0	0	0	0
8	5	1	0	1	0	1	1	0	1	1	1	0	0	0	0
9	5	1	0	1	0	1	1	1	1	1	1	0	0	0	0
10	5	1	1	1	1	1	1	1	1	1	1	0	1	0	0
11	5	1	0	1	1	1	1	1	1	1	1	0	1	0	0
12	5	1	0	1	1	1	1	1	1	1	1	1	1	1	0
13	5	0	0	1	1	1	1	1	1	1	1	1	1	1	0
14	5	0	0	1	1	1	1	1	1	1	1	1	1	1	0
15	5	1	0	1	1	1	1	1	1	1	1	1	1	1	0
16	5	1	1	1	1	0	1	1	1	1	1	1	1	1	0
17	6	1	1	0	1	0	1	1	1	1	1	1	0	1	0
18	6	1	1	0	1	0	1	1	1	1	0	0	0	1	0
19	6	1	1	0	1	0	0	1	1	0	0	0	0	1	0
20	6	1	1	0	1	0	0	1	1	0	0	0	0	1	0
21	6	1	1	0	1	0	0	1	1	0	0	0	0	1	0
22	6	1	1	0	1	0	0	0	1	0	0	0	0	1	0
23	6	1	1	0	1	0	0	0	0	0	0	0	0	0	0
24	6	1	1	0	0	0	0	0	0	0	0	0	0	0	0

Table 5.9 (continued)

hour	LTC	C1	C2	C3	C4	C5	C6	C7	C8	C9	C10	C11	C12	C13	C14
Optimal scheduling based on GA-Fuzzy [2]															
1	3	1	0	0	0	1	0	0	0	1	0	0	0	0	0
2	3	1	0	0	0	1	0	0	0	1	1	0	0	0	0
3	3	0	0	0	0	1	0	0	0	1	1	0	0	0	0
4	3	1	0	0	0	1	0	0	0	1	1	0	0	0	0
5	3	1	0	0	0	1	0	0	0	1	1	0	0	0	0
6	3	0	0	1	0	1	0	0	0	1	1	0	0	0	0
7	4	1	0	1	0	1	0	0	1	1	1	0	0	0	0
8	7	1	0	1	0	1	1	0	1	1	1	0	0	0	0
9	7	1	1	1	0	1	1	1	1	1	1	0	0	0	0
10	7	1	1	1	1	1	1	1	1	1	1	1	1	0	0
11	7	1	1	1	1	1	1	1	1	1	1	1	1	1	1
12	6	1	1	1	1	1	1	1	1	1	1	1	1	1	1
13	6	0	0	1	1	1	1	1	1	1	1	1	1	1	1
14	6	0	0	1	1	1	1	1	1	1	1	1	1	1	1
15	6	1	0	1	1	1	1	1	1	1	1	1	1	1	1
16	5	1	1	1	1	0	1	1	1	1	1	1	1	1	1
17	5	1	1	0	1	0	1	1	1	1	1	1	0	1	0
18	5	1	1	0	1	0	1	1	1	1	0	0	0	1	0
19	5	1	1	0	1	0	0	1	1	0	0	0	0	1	0
20	5	1	1	0	1	0	0	1	1	0	0	0	0	1	0
21	5	1	1	0	1	0	0	1	1	0	0	0	0	1	0
22	5	1	1	0	1	0	0	0	1	0	0	0	0	1	0
23	5	1	1	0	1	0	0	0	0	0	0	0	0	0	0
24	5	1	1	0	0	0	0	0	0	0	0	0	0	0	0

5.4.5. Analysis

The three optimization approaches present acceptable scheduling within the designated switching and operational constraints. All switching constraints (Table 5.9) are fully satisfied, voltage improvements are achieved (Fig. 5.6) and harmonic distortion is controlled (Fig. 5.8). According to Fig. 5.6, a slightly better voltage improvement is obtained by ACA as compared to GA. The hourly reduction of real power losses achieved by the scheduling is shown in Fig. 5.7 with a daily energy saving of 1789.80 kWh, 1859.50 kWh and 1810.50 kWh for GA, GA-Fuzzy and ACA, respectively. The overall optimization benefits are compared in Table 5.10.

Fig. 5.8 shows the THD reduction of the bus with the highest THD level (bus 81), before and after the optimization. As expected, the proposed ACA has successfully limited all THD levels below the selected maximum value of 5%. Inspecting the simulation results indicates that THD_V improvement by ACO is slightly better than both GA and GA-Fuzzy.

The overall optimization benefits of the three intelligent algorithms are provided in Table 5.10 and Fig. 5.8. The AC-based near-global optimal solution is achieved in 35 iterations while for the same operating conditions the counterpart GA and GA-Fuzzy approaches require 50 and 55 iterations, respectively. As expected, different runs of the each algorithm tend to generate slightly different results even for the same initial conditions. However, ACA is faster and requires less number of iterations and less computing time as compared to GA and GA-Fuzzy.

Table 5.10
Overall benefits of optimal dispatching based on GA, GA-Fuzzy and ACA

average optimization benefits	**optimization technique**		
	GA [1]	**GA-Fuzzy [2]**	**ACA (Fig. 3.7)**
voltage improvement (%)	9.11	9.66	9.20
total energy saving (kWh)	1789.8	1789.8	1810.5
THDv reduction (%)	5.22	5.36	5.26
required number of iterations	50	55	35
computing time (sec)*	11590	13328	10960

*) Pentium 4, Intel 3.0 GHz processor, 512 MB RAM, using Matlab ver. 7

5.4.6. Conclusions

This study investigates the performances of three intelligent system algorithms in solving the volt/VAr/ THD_V control problem for large distribution systems. The optimization approaches tested are GA, GA-Fuzzy and ACA. Simulation results are compared for the distorted IEEE 123-bus system. Main conclusions are:

GA, GA-Fuzzy and ACA have effectively achieved the optimization goals in the presence of harmonics.

The developed ACA can successfully mitigate voltage THD_V distortions below the IEEE-519 and IEC-61000 recommended level of 5%, keeps voltage variations at all buses within the designated levels (0.95 and 1.05pu) and reduces power losses.

Compared with the GA and GA-Fuzzy, the developed ACA results in slightly better quality of solution in terms of the convergence (Table 5.8), voltage profile (Fig. 5.6) and THD reduction (Fig. 5.8).

As with the GA and GA-Fuzzy, proper selection of optimization parameters (weighting functions, initial parameters, value of initial pheromone and number of iterations) will improve the solution and reduce computing time.

Results show that all three intelligent algorithms perform better than ad-hoc placements of reactive power sources but differ in convergence, computational effort and accuracy of solutions. It is hoped that the results presented in this paper will help consolidate the research directions in this area of distribution system optimization using intelligent algorithms.

5.5. Optimal Scheduling of modified IEEE- 31 bus System

In this section, a relatively simple and inexpensive approach is presented to improve the voltage profile and control the power quality of smart grids. For moderate numbers of smart appliances, optimal dispatch of the existing LTC and capacitor banks are performed using GA. For grids with high penetration of smart appliances, a passive filter bank is connected at the worst bus prior to the rescheduling of switching devices. The decoupled harmonic power flow (DHPF) algorithm is used as the backbone of the optimization and filter tuning problems and case studies are presented based on the IEEE 31-bus 23 kV system

5.5.1. System Data

To illustrate the harmonic mitigation approach of Figure 5.9, the IEEE 31-bus 23 kV distribution systems is modified to include a residential feeder with high penetration of Plug in Electric Vehicles (PEVs) and another serving an industrial area with nonlinear loads (Fig. 5.10). A 250 kVA 23 kV/415(240) V distribution transformer is also placed at bus 4 feeding high-penetration PEV nonlinear loads and linear loads (buses 23-28) at the customer side. Figure 5.11 shows waveform of the injected current of the PEV charger (Table 5.11).

.

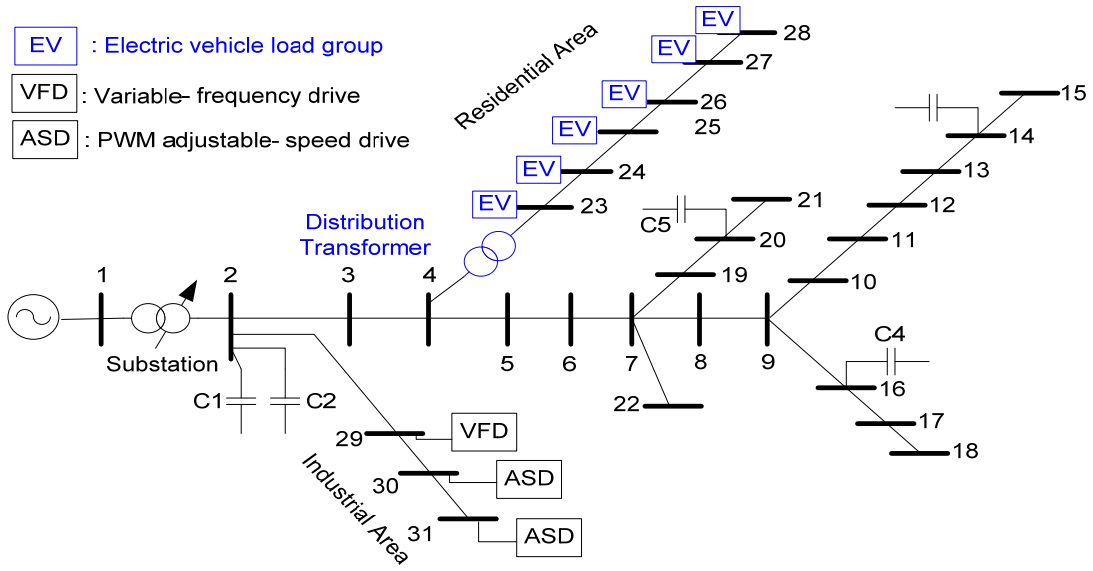

Fig. 5.10. Modified IEEE 31-bus 23kVdistribution system with residential and industrial feeders [11-12].

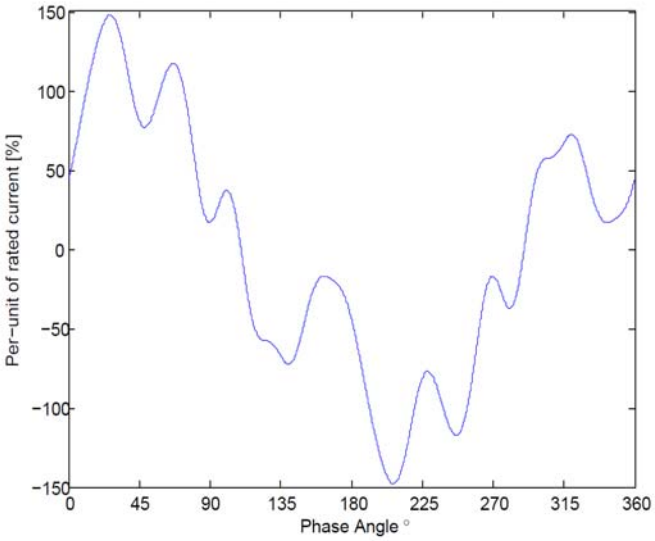

Fig. 5.11. Waveform of the injected current for PEV charger (Table 5.11)

Table 5.11
Typical Harmonic current contents of industrial loads [1] and electric vehicle chargers [55]

Harm. order h	six-pulse VFD		PWM-ASD		PEV	
	Mag. [%]	Phase [deg]	Mag. [%]	Phase [deg]	Mag. [%]	Phase [deg]
1	100	0	100	0	100	-26
5	23.52	111	82.8	-135	25	-94
7	6.08	109	77.5	69	17	-67
11	4.57	-158	46.3	-62	9	-67
13	4.20	-178	41.2	139	5	-46
THDi	7.1 %		25..2 %		31.9%	

5.5.2. Passive Filter Bank for Harmonic Mitigation

The above-mentioned optimal dispatch formulation will limit harmonic voltages and currents of most distorted distribution systems since capacitor banks in conjunction with the line inductances act as filters. However, for high penetration of nonlinear loads and smart appliances, passive (L-C-R) filter placement might also be required.

The configuration and complexity of the filter depends on harmonic spectrum and nature of the distortion [56]. Passive filters are the best candidates for time invariant nonlinear loads. These filters are inexpensive compared with most other mitigating devices. Passive filters are composed of only passive elements (inductance, capacitance, and resistance) tuned to the harmonic frequencies. In practice, passive filters are added to the system starting with the lowest-order but significant current harmonic (e.g., installing a seventh-harmonic filter usually requires that a fifth-harmonic filter also be included).

Since drive systems and PEVs mainly inject low-order harmonics, a hybrid filter block consisting of a number of band-pass filters tuned to dominating harmonic frequencies [56] will be used (Fig. 5.12). The resonant frequency of each shunt branch is:

$$\omega_h = 2\pi hf = 1/\sqrt{L_f^h C_f^h} \tag{5-1}$$

where h is the order of harmonic that is being attenuated, f is the fundamental frequency, L_f^h and C_f^h are filter inductor and capacitor, respectively.

5.5.3. Solution Algorithm

The flow chart of the harmonic mitigation approach by performing optimal dispatch and/or passive harmonic filter placement at the worst buses of the smart grid is presented in Figure 5.12. It consists of the following steps:

Step 1: Input line and load data including the harmonic orders, magnitudes and phase angles of the harmonic currents injected by industrial loads and smart appliances. Assume the number of load intervals (e.g., 4).

Step 2: Model the nonlinear loads and smart appliances with decoupled harmonic current sources

Step 3: Find the optimal load interval divisions using GA.

Step 4: Use GA for optimal dispatch of LTC and switched capacitors.

Step 5: Run DHPF, identify the worst bus (e.g., the bus with the highest voltage THD distortion) and calculate the overall voltage THD_V.

Step 6A: If $THD_V < 5\%$, print the optimal schedules of the LTC and shunt capacitors for the next 24 hours and stop.

Step 6B: If THDv>5%, place a passive filter bank at the worst bus (tuned to dominating low - order harmonics). Go to *Step 3*.

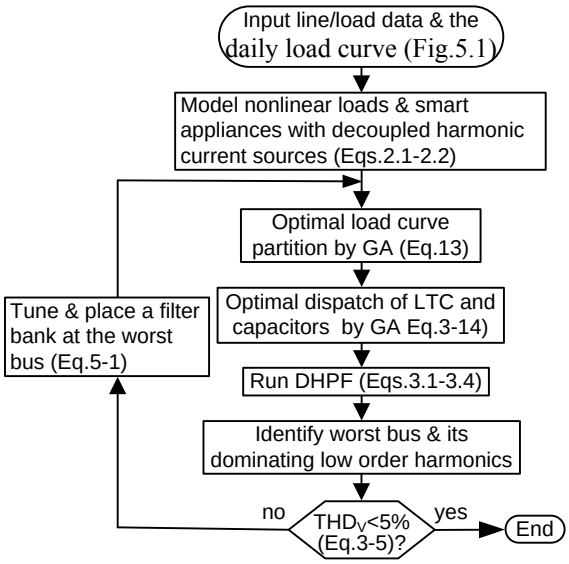

Fig. 5.12. Flow chart of the harmonic mitigation approach for smart grids with high penetration of smart appliances

5.5.4. Simulation Results

Case 1: Harmonic Mitigation of IEEE 31-Bus Distribution System with Low Penetration of PEVs.

Simulations are performed for the IEEE 31-bus system with 120 PEV chargers grouped at 6 nodes along the residential feeder. Each charger is rated at 1.3 kW (5.3A at 240 Vac single-phase). The industrial feeder consists of two large nonlinear loads (a variable-frequency drive (VFD) rated at 450 kW, 439 kVAr and a PWM based adjustable-speed drive (ASD) rated at 350 kW, 175 kVAr, placed at buses 29

and 30, respectively). The typical daily load curve of Figure 3.4 in Chapter 3 is used for all linear and nonlinear loads. Simulation results before and after performing genetic optimal dispatch is presented in Figures 5.13-5.15 showing considerable improvement in terms of voltage profile, losses and THDv.

Note that for this case, the overall average THD value, as well as, all individual bus THD levels are limited below 5%. Therefore, there is no need for passive filters. However, the voltage profile is not perfectly controlled below the limit of 0.95 pu.

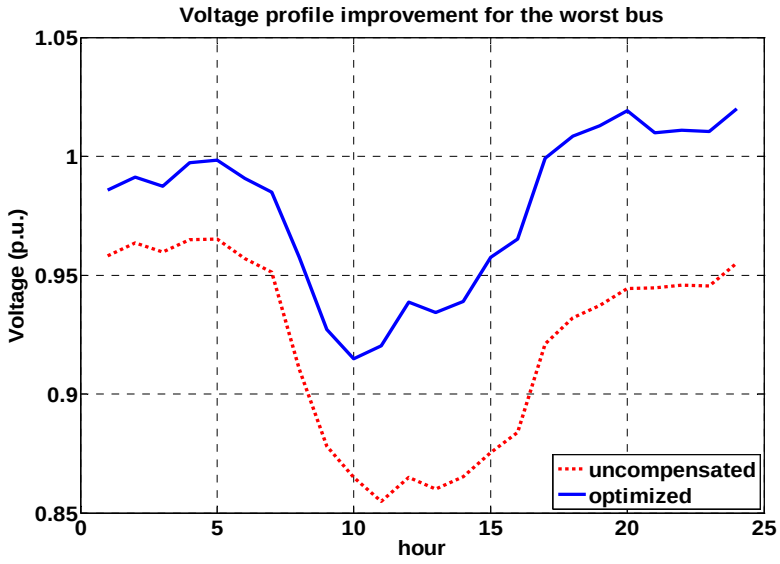

Fig. 5.13. Improvement of voltage profile at the worst bus (Fig. 5.9, bus 16) due to optimal dispatch of LTC and capacitors for the IEEE 31-bus system with low penetration of PEVs

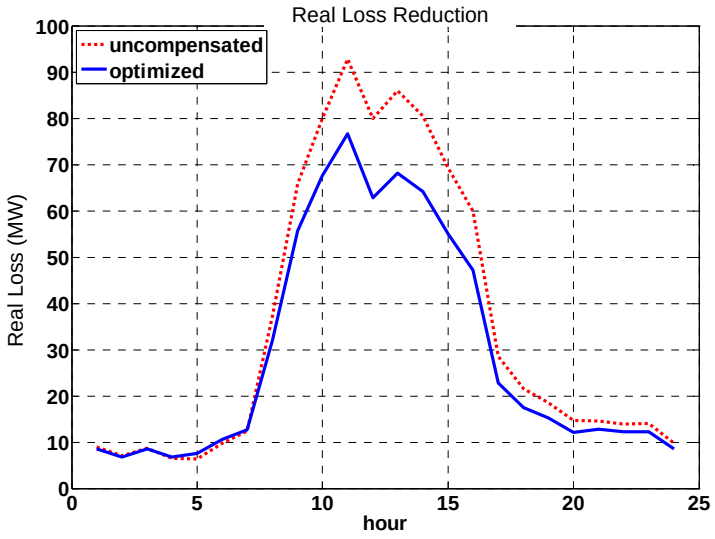

Fig. 5.14. Reduction in real power losses due to optimal dispatch of LTC and capacitors for the IEEE 31-bus system with low penetration of PEVs.

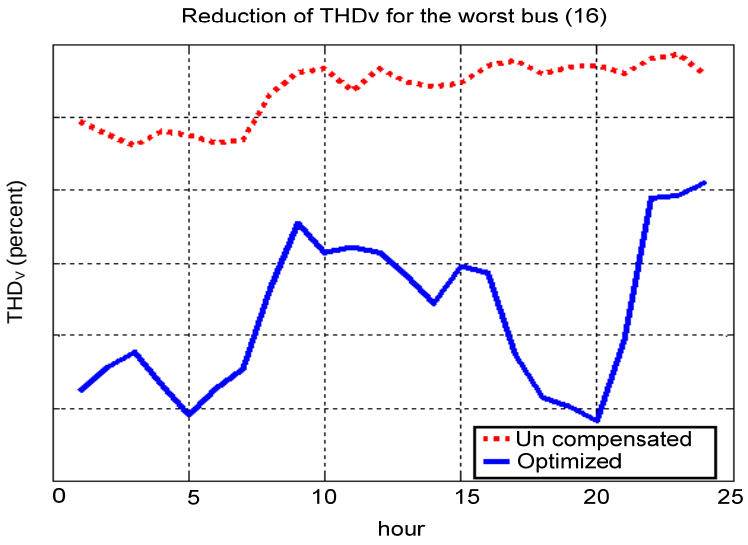

Fig. 5.15.Improvement of THDv at the worst bus (16) due to optimal dispatch of LTC and capacitors for the IEEE 31-bus system with low penetration of PEVs.

Case 2: Harmonic Mitigation for IEEE 31-Bus Distribution System with High Penetration of PEVs

The number of PEVs is increased to 240 and each charger is rated at 1.3 kw (5.3 Amps at 240 Vac single-phase). The industrial feeder consists of three large nonlinear loads; one VFD (rated at 675 kW and 439 kVAr) and two ASDs (each rated at 350 kW, 175 kVAr), placed at buses 29, 30 and 31, respectively. Simulation results are presented in Figures 5.16-5.18. For this case, rescheduling of the switching devices cannot fully control harmonic distortions and reduce the THD_V to 5%. However, after the placement of a shunt passive filter bank at the worst bus (Fig. 5.10, bus 28) the overall system THD_V is limited to 1.75%.

Using the iterative algorithm of Fig .5.12, the passive filter bank is placed on bus 28 (e.g., the worst bus) and tuned at four dominating harmonics (e.g., 5^{th}, 7^{th}, 11^{th}, and 13^{th}). The fundamental frequency is f_1=50Hz and filter components are: R_F=1Ω, L_F=100mH , $C^{(5)}_F$=2.07□μF, $C^{(7)}_F$=0.84μF, $C^{(11)}_F$=0.6 μF, and $C^{(13)}_F$ =0.35 μF.

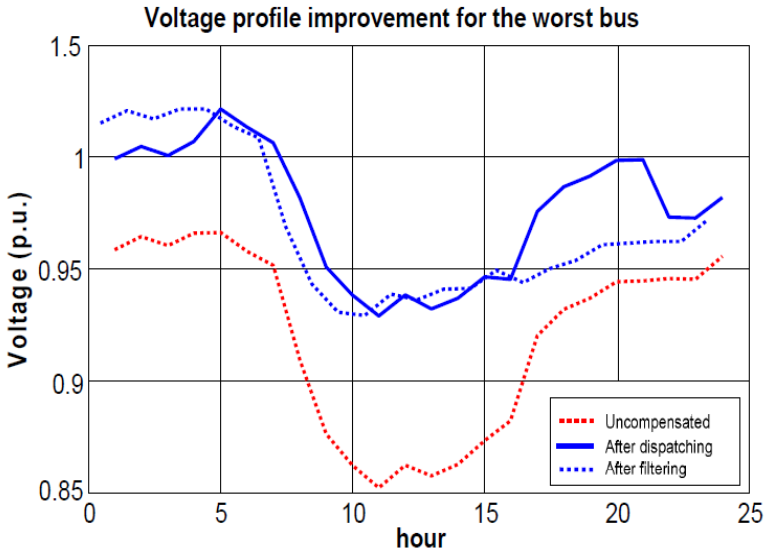

Fig. 5.16. Improvement of voltage profile at the worst bus (Fig. 5.9, bus 28) due to optimal dispatching (of LTC and capacitors) and/or filtering.

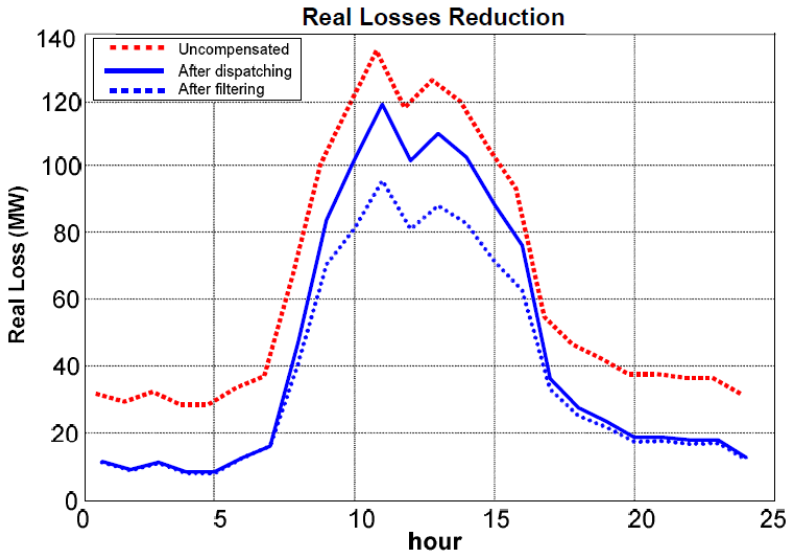

Fig. 5.17. Reduction in real power losses due to optimal dispatching (of LTC and capacitors) and/or filtering.

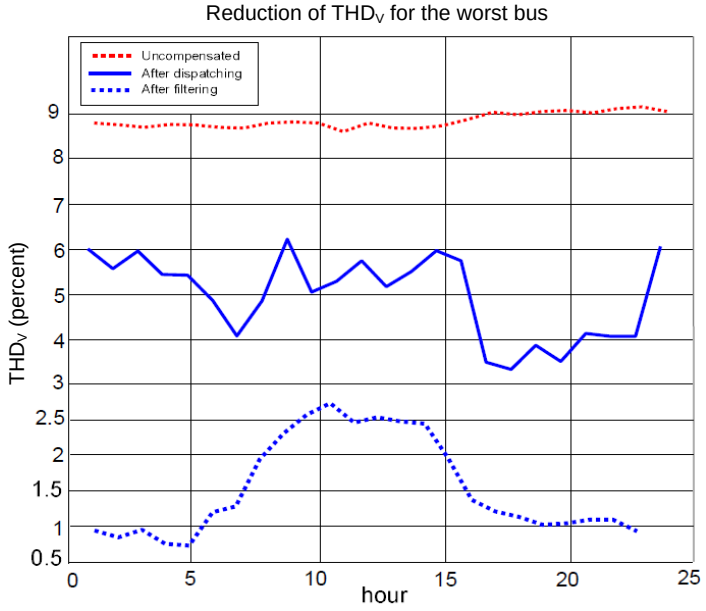

Fig. 5.18. Improvement of THDv at the worst bus (Fig. 5.9, bus 28) due to optimal dispatching (of LTC and capacitors) and/or filtering

Table 5.12
Summary of Simulation Results for Case 2 (Modified IEEE 31-Bus System of Fig. 5.10). Before and After Optimal Dispatch (of LTC and Capacitors) and/or Filtering

	before dispatching and/or filtering		after dispatching		after dispatching and then filtering	
	min [pu]	max [pu]	min [pu]	max [pu]	min [pu]	max [pu]
|V| [rms]	0.855 at bus 15	0.963 at bus 1	0.942 at bus 15	1.029 at bus 2	0.942 at bus 15	1.032 at bus 1
THDv [%]	8.528 at bus 15	9.12 at bus 28	3.872 at bus 27	6.492 at bus 16	0.677 at bus 27	2.79 at bus 23
system THDv [%]	8.82%		5.20%		1.75%	

5.5.5. Conclusions

This chapter aims at improving power quality of smart grids with high penetration of industrial and residential nonlinear loads. It proposes optimal dispatch prior to passive (or active) filter installation. An iterative approach based on DHPF and GA is proposed and implemented. Main conclusions are:

- For smart grids with low penetration of nonlinear loads, harmonic distortions can be compensated by optimal dispatching if THD_V is included as a GA constraint.

- For smart grids with moderate harmonic pollution levels, depending on the types, durations, ratings, numbers and positions of smart appliances, there might be a chance to control the THD_V level by rescheduling the switching devices.
- For smart grids with high penetration of smart appliances, some compensation approach such as passive filter installation is required. However, to reduce the rating and the cost of compensation, it is recommended to perform optimal dispatch of LTC and shunt capacitors prior to the compensation.
- The proposed iterative mitigation method may be applied to other harmonic compensation approaches such as active and hybrid filtering.

5.6. Discussion

As with all optimization problems, computation time is one of the most important issues in the optimal dispatch problem. This is especially important in harmonically distorted distribution systems with nonlinear loads requiring many runs of the harmonic load flow algorithm within the iterative optimization algorithm.

The detailed analyses and simulations in this chapter indicate that the three intelligent approaches based on GA, GA-Fuzzy and ACA can successfully perform the optimization dispatch problem under non-sinusoidal operating conditions. However, the proposed ACA has better convergence characteristics and requires considerably fewer numbers of iterations and less computing time (Table 5.10) as compared with the GA and GA-Fuzzy methods.

Additionally, taking harmonics into account will complicate the optimization process and increase the required computing time due to consideration of harmonic orders. Harmonic power flow is run over 24 hours for the optimal scheduling which requires longer computation time in large distributed systems such as the IEEE 123-bus system presented in this chapter. For verification purpose, every generated schedule presented in this thesis has been manually checked by running the schedules for the simulated systems on an hourly basis. It is confirmed that the results generated by GA, GA-Fuzzy and ACA are quite accurate.

CHAPTER SIX
ANT COLONY BASED OPTIMAL DISPATCH OF A SMART GRID

This chapter presents the application of ant colony optimization in a smart grid and proposes a novel load management algorithm for the coordination of Plug-In Electric Vehicle (PEV) Chargers to minimize losses and improve voltage profile.

So far there has been significant research in integrating customer-demand-side management into smart grids to improve the system load profile and reduce peak demand [1-3, 28-30]. However, there are growing concerns and issues about the relatively high rating, nonlinearities and charging regimes associated with PEVs, as well as their impacts on the overall daily load pattern for residential systems [27]. An unexpected number of simultaneous PEV charger loads during the peak hours may alter the overall residential daily load curve, increase system losses, deteriorate power quality, cause voltage fluctuations and overloading problems. Voltage deviations may cause reliability problems that should not be underestimated in order to avoid malfunctioning of electric appliances [57]. In order to investigate and overcome the above-mentioned potential problems, this research aims to simulate and optimize a smart grid configuration consisting of a high voltage distribution system serving nonlinear industrial nodes connected to a number of low voltage residential feeders populated with PEVs.

In Section 6.1, the proposed ACA of Chapter 3 is implemented based on the distribution part of the smart grid to minimize losses and improve voltage profile relying on the optimal dispatch of LTC and switched shunt capacitors. For further improvement of the smart grid operation, Section 6.2 proposes a Smart Load Management (SLM) algorithm for the coordination of residential PEV charging activities that will further reduce the overall losses and improve the voltage profile. The impacts of different charging regimes (random and coordinated), charging periods (peak and off-peak) and PEV penetration (low, moderate and high) on the performance of a smart grid considering load variations over a 24 hour period are also analyzed and simulated.

6.1. The 449-Bus Distribution/Residential Smart Grid Configuration

A detailed smart-grid system test topology (Fig. 6.1) is developed and studied to show the impact of proposed dispatch ACA of Chapter 3 and the proposed SLM of Section 6.3 on the smart - grid losses, voltage profile and THD_V.

6.1.1. System Topology

The selected system (Fig. 6.1) is a modification of the IEEE 31-bus 23 kV distribution test system [22] combined with several residential low voltage (LV) 415 V networks based on real system data of a neighbourhood in Western Australia. Each LV feeder consists of 19 nodes representing customer households with selected nodes assigned PEVs, priority and charging zone (Table 6.1). A total of 22 LV 19 node feeders are implemented and supplied from the high voltage (HV) main buses via 23kV/415V 100 kVA distribution transformers. The total number of nodes of this system is 449 (31 HV nodes and 418 LV nodes). The system data are listed in Tables 6.2 and 6.3.

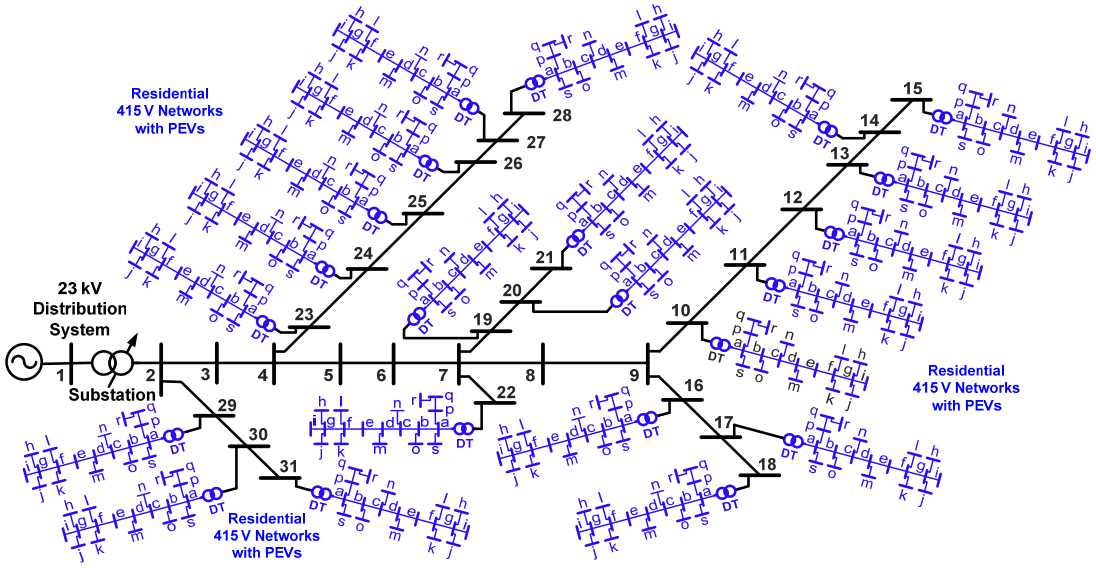

Fig. 6.1. The 449 bus smart grid distribution/residential system topology consisting of the IEEE 31-node 23 kV distribution system with several 415 V residential feeders. Each low voltage residential network has 19 nodes representing customer households with varying penetrations of PEVs (Table 6.1).

6.1.2. PEV Energy Requirements

For realistic modelling PEV charging loads, the battery energy contents are of importance to determine reasonable charging profiles. PEV battery capacities typically range from a few kWhs to over 50 kWh [1-4]. For this study, a 10 kWh battery capacity per PEV is selected because it is expected that the lower end of battery sizes are more affordable and more likely to initially dominate the market.

In order to optimize PEV battery life, deep cycle batteries with a depth of discharge (DOD) of 70% rated battery life is assumed resulting in an available capacity of 7 kWh that the charger must deliver. Battery chargers have some losses and therefore the energy requirement from the grid is actually greater than the stated battery capacity. A typical battery charger efficiency of 88% is assumed thereby requiring a total of 8 kWh of energy from the grid to charge a single PEV.

6.1.3. PEV Battery Chargers

In practice, PEV battery chargers will have to be rated high enough to charge batteries of these sizes in reasonable time periods. However, limitation of household wiring must also be considered. A standard single-phase 240V outlet (Australia) can typically supply a maximum of 2.4 kW. There are also 15A and 20A outlets (single-phase and three-phase) which can supply approximately 4 kW and 14.4 kW, respectively. For this analysis, a fixed charging power of 4 kW is selected because this is commonly available in most residential households with single-phase power systems without having to upgrade wiring.

6.1.4. Load Profiles

A typical residential load curve based on actual recording from a distribution transformer (in Western Australia) is used to model the domestic load variations (without PEV charging) at each house over a 24 hour period (Fig. 6.2). The peak power consumption of a house is assumed to be on average 2 kW with a power factor of 0.9 lagging.

6.1.5. PEV Penetration Levels

In order to cover the widest range of plausible PEV charging scenarios in the near and long-term future, four different PEV penetration levels (16%, 32%, 47% and 63%; Table 6.1) are simulated for each charging approach. These penetration levels are defined to be the proportion of nodes with PEVs to the total number of LV residential nodes (excluding transformer LV node). A maximum of one PEV per household is assumed.

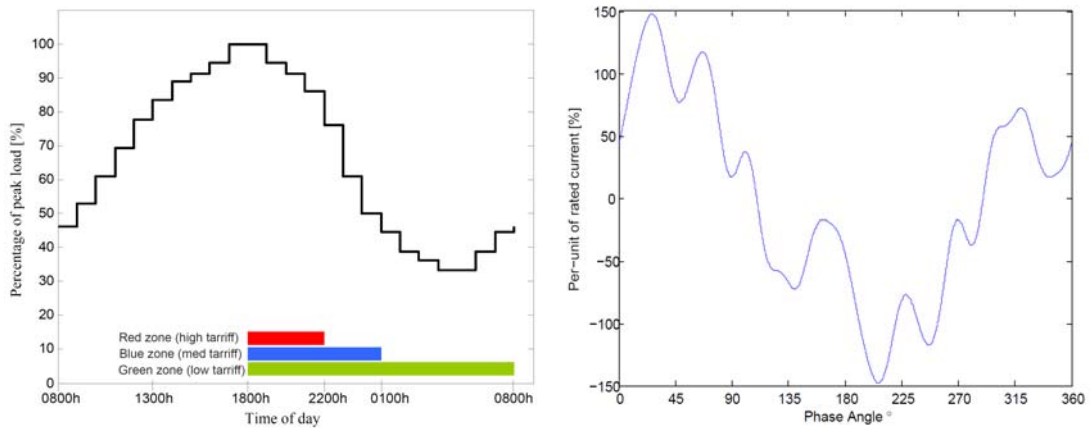

(a) (b)

Fig. 6.2. Daily residential load curve; (b) Non-sinusoidal waveform of input current for PEV charger (Table 6.4)

Table 6.1
Designated PEV penetration levels and assigned priorities for charging time zones
(Red=High priority, Blue=Medium priority, Green=Low priority).

19 node system	PEV penetration levels			
	16%	32%	47%	63%
a				
b				
c				
d				
e				
f				
g				
h				
i				
j				
k				
l				
m				
n				
o				
p				
q				
r				
s				

*) Boxes with no color indicate nodes with no PEVs present

Table 6.2
Linear and nonlinear (PEV) loads of the typical low voltage residential system (Fig. 6.1)

linear and PEV load		power	
bus	name	kW	kVAr
1 to 19	linear loads	2	1.7
selected buses	PEV charger	4.0	0

Table 6.3
Line parameters of the low voltage residential system (Fig. 6.1)

LINE		line resistance R [Ω]	line reactance X [Ω]	LINE		line resistance R [Ω]	line reactance X [Ω]
from bus	to bus			from bus	to bus		
a	b	0.0415	0.0145	F	l	1.3605	0.1357
b	c	0.0424	0.0189	D	m	0.140	0.0140
c	d	0.0444	0.0198	C	n	0.7763	0.0774
d	e	0.0369	0.0165	B	o	0.5977	0.0596
e	f	0.0520	0.0232	A	p	0.1423	0.0496
f	g	0.0524	0.0234	P	q	0.0837	0.0292
g	h	0.0005	0.0002	Q	r	0.3123	0.0311
g	i	0.2002	0.0199	A	s	0.0163	0.0062
g	j	1.7340	0.1729	Distribution transformer reactance= 0.0654 Ω			
f	k	0.2607	0.0260				

Table 6.4
Typical line current harmonic content of a PEV charger [69]

harmonic order h	magnitude [%]	phase angle [degree]
1	100	-26
5	25	-94
7	17	-67
11	9	-67
13	5	-46
THD_i	31.9%	

6.1.6. Designated PEV Priorities

Within the penetration levels of Table 6.1, the PEVs are grouped into priority time zone groups (e.g., red, blue and green zones; Fig. 6.2). A realistic breakdown of priorities is assumed by having the majority of the PEVs owners subscribing to green and blue zone priorities, respectively. This is because the lower pricing of blue and green zones will be more attractive to PEV owners compared to higher tariffs in the red zone charging. For each penetration level, the assumed priorities are proportioned randomly to PEV nodes in each LV residential network as shown in Table 6.1.

6.2. AC Based Optimal Dispatch of Smart Grid

The proposed ant colony optimization algorithm of Chapter 3 is employed to show its performance and ability in smart grid optimization of losses, voltage profile and harmonic distortion. The AC based optimal dispatch of LTC and switched shunt capacitors are performed for the 449-bus smart grid system of Fig. 6.1 with the following modifications:

- Each 22 low voltage feeder is replaced with a large PEV nonlinear load representing the conventional linear residential load and the PEV charging activities under the worst scenario. The fundamental active and reactive power consumption of each large PEV nonlinear load are 0.024 pu and 0 pu (base: 100KVA), respectively.
- The current harmonic components of the large PEV nonlinear load (based on the non-sinusoidal waveform of Fig. 6.2b are listed in Table 6.4.

Simulation results are shown in Table 6.5 and Figs. 6.3 to 6.5. Analyses of the results indicate that:

- The new LTC and capacitor schedules (with the consideration of injected PEV current harmonics) are different from the conventional schedules (assuming linear PEV charger characteristics).
- The voltage profiles are considerably improved and are kept within the designated lower and upper limits of 0.9 pu and 1.0 pu, respectively (Fig. 6.3).
- There is a notable reduction in the total system losses due to the reactive power support of the shunt capacitors (Fig. 6.4).
- The THD_V distortion is reduced from about 12% to about 4% (Fig. 6.5).

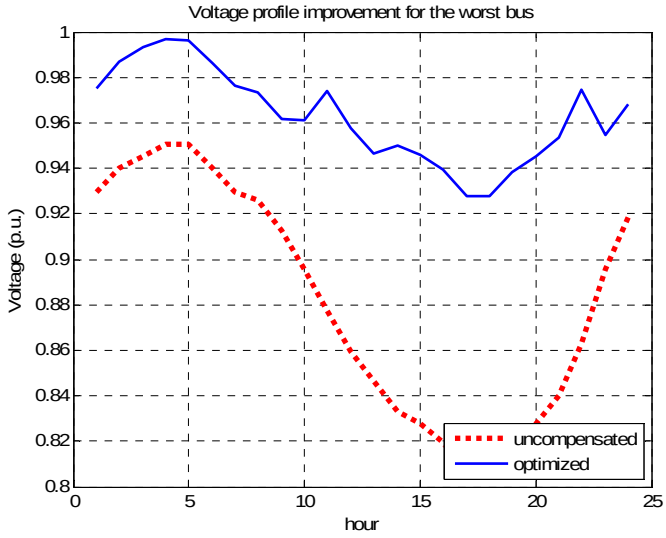

Fig. 6.3. Voltage improvement of the worst bus (bus 15) for the simplified 449-bus smart grid of Fig. 6.1 based on the proposed ACA optimization of Chapter 3.

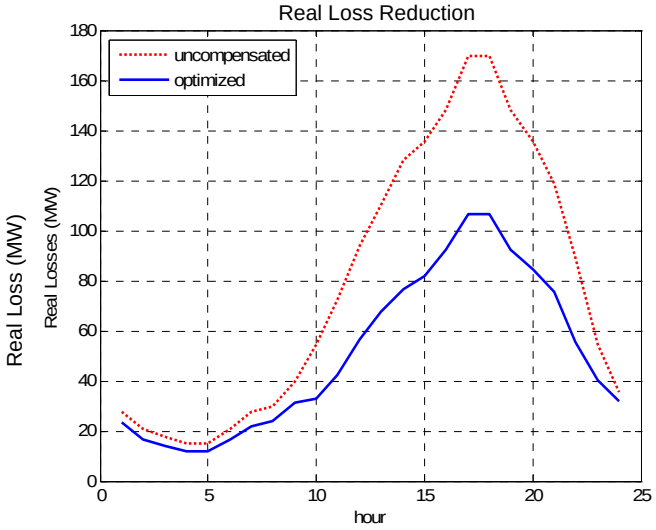

Fig. 6.4. Power loss minimization for the simplified 449-bus smart grid of Fig. 6.1 based on the proposed ACA optimization of Chapter 3.

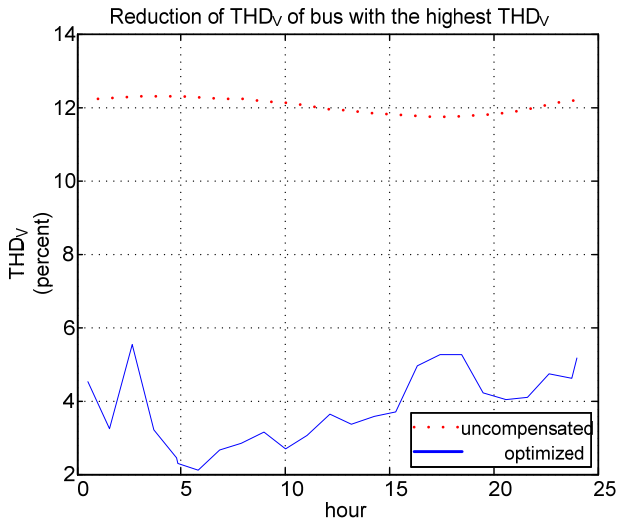

Fig. 6.5. THD voltage distortion at the worst bus (bus 26) for the simplified 449-bus smart grid of Fig. 6.1 based on the proposed ACA optimization of Chapter 3.

Table 6.5
AC based optimal scheduling of LTC and switch shunt capacitors for the simplified 449-bus smart grid of Fig. 6.1 considering the harmonic distortions caused by the PEV chargers.

hour	**optimal schedule of the simplified 449-bus smart grid (Fig. 6.1) by ACA**							
	LTC	**C1**	**C2**	**C3**	**C4**	**C5**	**C6**	**C7**
1	4	1	0	0	0	0	0	1
2	4	1	0	0	0	1	0	1
3	4	0	0	0	0	1	0	1
4	4	0	1	0	0	1	0	1
5	4	1	1	0	0	1	0	1
6	4	1	1	0	0	1	0	1
7	4	1	1	0	0	1	0	1
8	4	1	1	0	0	1	0	1
9	4	1	0	0	0	1	1	1
10	4	1	0	1	1	1	1	1
11	6	1	0	1	1	1	1	1
12	6	1	0	1	1	1	1	1
13	6	1	1	1	1	1	1	1
14	7	1	1	1	1	1	1	1
15	7	1	1	1	1	1	1	1
16	7	1	0	1	1	1	1	0
17	7	1	0	1	1	1	1	0
18	7	1	0	1	1	1	1	0
19	7	1	1	1	1	1	1	0
20	7	1	1	1	1	1	1	0
21	7	1	1	1	1	0	1	0
22	7	0	1	1	1	0	1	0
23	4	1	0	1	0	0	1	0
24	4	1	0	0	0	0	0	0

6.3. Smart Load Management (SLM) for PEV Coordination

A novel load management solution is proposed for coordinating the charging of multiple Plug-in Electric Vehicles (PEVs) in a smart grid system. PEVs are becoming popular as a low emission mode of transportation over conventional petroleum based vehicles. Utilities are becoming concerned about the potential stresses, performance degradations and overloads that may occur in distribution systems with multiple domestic PEV charging activities. Uncontrolled and random PEV charging can cause increased power losses, overloads and voltage fluctuations, which are all detrimental to the reliability and security of newly developing smart grids. Therefore, a new smart load management (SLM) control strategy is proposed and developed for coordinating PEV charging based on minimizing power losses and improving voltage profile in smart grids. The developed SLM approach takes into consideration the PEV owner's preferred charging time zones based on priority selection. Simulation results are presented to demonstrate the performance of SLM for the modified IEEE 23 kV distribution system connected to several low voltage residential networks populated with PEVs.

To demonstrate the improvements in smart grid performance, SLM is simulated with a detailed system topology consisting of a high voltage feeder with several integrated low voltage-residential networks populated with PEVs. Simulation results including total power consumption, system losses and voltage profile are presented for (un)coordinated charging with PEV penetration of 16%, 32%, 47% and 63% considering three designated time zones; red: 1800h-2200h, blue: 1800h-0100h, and green: 1800h-0800h.

6.3.1. Overview of SLM

As an alternative to PEV chargers which randomly and immediately operate when first plugged in, or after some fixed time delay, the proposed SLM will decide which PEVs will charge at what time. PEV charger control can be achieved through the forthcoming smart-grid communications infrastructure by sending and receiving signals to individual PEV chargers. This means that PEV charging control would be taken out of the hands of the owner and scheduled automatically. The proposed SLM

will perform loss minimization based on Eq. (6-3) and the system constraints (Eqs. 6-1, 6-2). Furthermore, SLM also takes into consideration existing load variations over a 24 hour cycle while considering PEV owner preferences for charging time zone and priority. Based on this and load flow computed outputs, SLM assigns charging schedules for individual PEVs to maximize smart-grid operational performance.

6.3.2. Problem Formulation for PEV Coordination

This section describes the formulation of the PEV charging coordination problem. The problem is deconstructed into a series of system constraints and an objective function necessary for the improvement of performance and economy of smart grids.

System Constraints:

The voltage constraints of the distribution system will be considered by setting the upper and lower limits to correspond to voltage regulation limits typically set by utilities. In this chapter, the voltage limits are set to +/- 10% ($V^{\min} = 0.9\,pu$ and $V^{\max} = 1.1\,pu$) which is typical of many distribution systems

$$V^{min} \le V_k \le V^{max} \quad for\ k = 1,..,n. \tag{6-1}$$

The second constraint is for setting a ceiling limit for the total maximum system demand of the distribution system to prevent an overload condition from PEV charging. Therefore, the total power consumption is limited to the peak demand value that would normally occur without any PEVs.

$$P_{max\,demand} = \sum_{k} P_k^{load} \le P_{total\,limit} \tag{6-2}$$

Objective Function for PEV Coordination:

The selected objective function for the PEV charging coordination problem is based on the minimization of total system power losses over 24 hours. The justification for this is that a smart-grid economy will largely depend on the cost of energy that would be expended on cable and transformer losses. Therefore, the following objective function is defined.

$$min\ W_{loss} = \sum_{h=chgStart}^{chgEnd} P_h^{total\,loss} \tag{6-3}$$

The power losses of the distribution system are computed from the Newton-based power flow outputs. The power loss in each line section between nodes *k* and *k+1* is

$$P_{loss(i,i+1)} = R_{i,i+1}\left(\left|V_{i,i+1} - V_i\right|\left|y_{i,i+1}\right|\right)^2 \quad (6\text{-}4)$$

and the total power loss for an *n* bus system is

$$P_{loss} = \sum_{k=0}^{n-1} P_{loss(k,k+1)} \quad (6\text{-}5)$$

6.3.3. Charging Zone and Priority Scheme

The developed SLM allows PEV owners to indicate their preferred charging time zone (Fig. 6.6). The SLM will try to accommodate these preferences while considering the loss minimization objective function and system constraints.

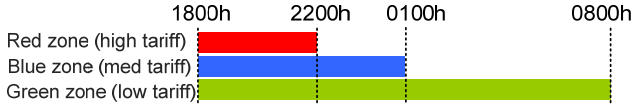

Fig. 6.6. Subscription options of charging time zones for PEV owners.

Three charging zones have been defined for this study:

- Red charging zone (1800h-2200h)- coinciding with most of the on-peak period and is designated for (high priority) PEV owners wanting to charge their PEVs as soon as possible on return from work in order to have their vehicles ready for use later in the evening. These PEV owners desiring to charge during this period of high demand will be charged a higher tariff rate.
- Blue charging zone (1800h-0100h) - is for (medium priority) consumers that prefer to charge their vehicles at partially off-peak periods and pay a lower tariff rate.
- Green charging zone (1800h-0800h) - is the period that most PEV charging will take place since most (low priority) consumers will require their vehicles fully charged for use throughout the next day. Charging off-peak will be highly encouraged by setting the cheapest tariff rates.

Note that all charging zone periods begin at 1800h and are allowed to overlap for some duration. This makes it possible for SLM to accommodate medium and low priority subscribers the opportunity to charge their vehicles earlier if possible. That is, after scheduling higher priority subscribers, lower priority customers can be served if there is enough capacity without violating system constraints.

6.3.4. The Proposed Smart Load Management (SLM) Algorithm

A MATLAB based algorithm has been developed to perform PEV scheduling based on SLM (Fig. 6.7). The algorithm begins by first reading the input parameters (e.g., bus and branch impedance data, nodes with PEVs, designated priority time zones, load profiles for PEV chargers and residential loads as well as system constraints) and performing initialization (e.g., selecting the highest priority group, time zone and PEV).

The main program loop is initiated progressing from high to low PEV priority groups (e.g., red to green zone). Within the selected priority group, individual PEVs are temporarily activated to determine system performance at all possible PEV node and charging time combinations within that priority charging time zone. From these combinations, the algorithm selects the PEV within the group and the charging start time resulting in the minimum system losses, taking into consideration the charging duration, and current demand level. The physical node location at which PEV charging occurs is an important factor as it impacts the load flow, power losses in the cables and system voltage profile. Therefore, the SLM determines the PEV node and charging time that will result in the least system losses (Eq. 6-3). If at any time the load flow indicates a constraint violation at any node (Eqs. 6-1, 6-2), the algorithm will try the next possible charging start time such that the constraints are satisfied. Therefore, it may not be possible for all PEV owners to be accommodated in their preferred charging zones and must be deferred to the next possible hour. Once it has been determined which PEV node in that priority group can begin charging and at what time resulting in minimum system losses, the selected PEV scheduling is permanently assigned and the system load curve updated ready for the next iteration. This process is repeated for all nodes in that priority group before advancing to the next priority charging zone (e.g., blue zone subscribers). At the end of this process,

the SLM algorithm arrives at individual schedules assigned to all PEV chargers. The program then exits the main loop and computes the 24 hour load flow to print new system performances (e.g., all node voltage profiles and power losses).

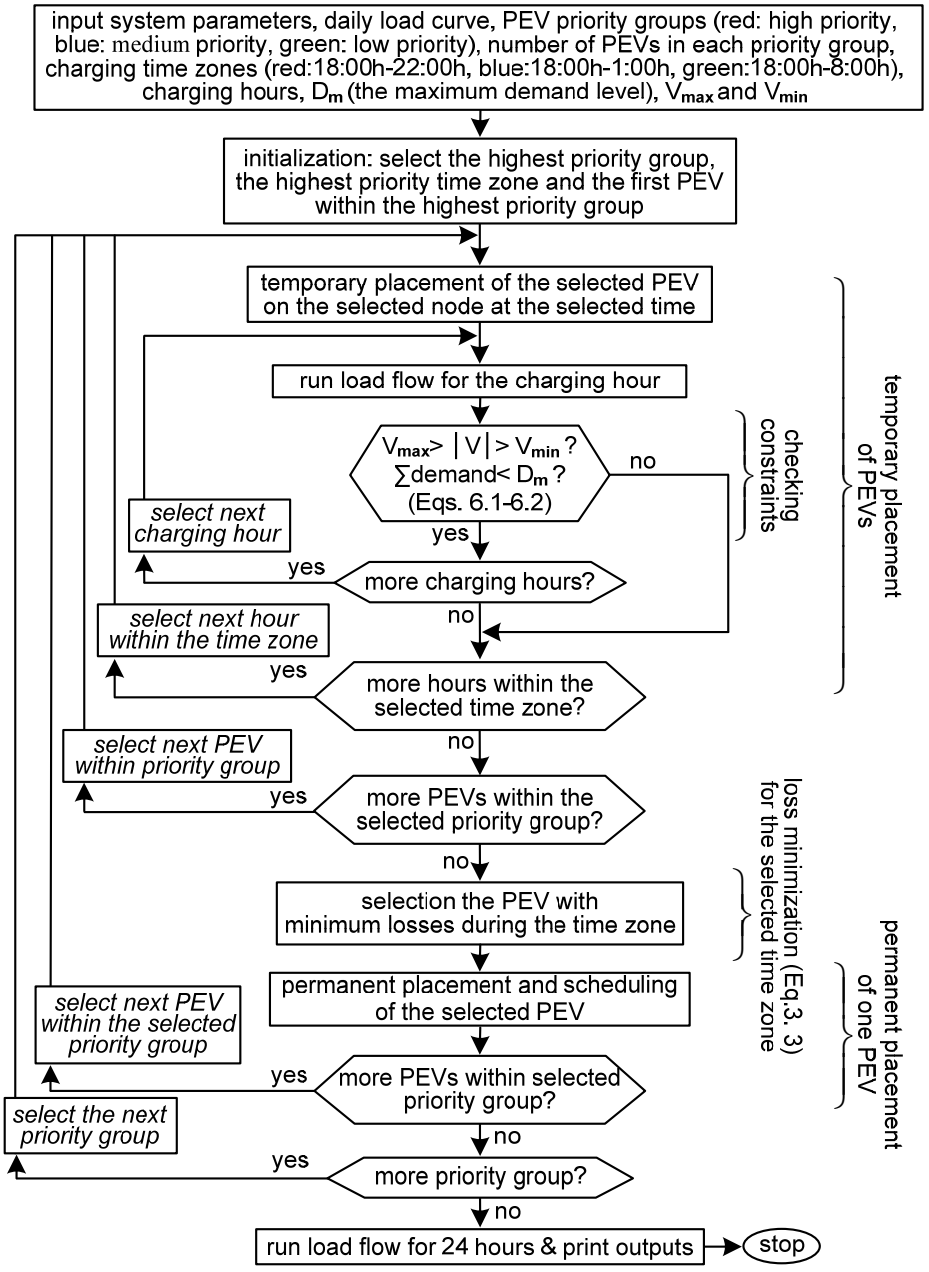

Fig. 6.7. SLM algorithm for coordinated PEV scheduling considering system losses, voltage profile and peak demand value.

6.3.5. Results and Discussion

Simulation results for different PEV charging scenarios for the smart-grid system with residential feeders (Fig. 6.7) are presented and compared in Figs. 6.8-6.24 and Tables 6.5 and 6.6. Impacts of randomly uncoordinated PEV charging versus coordinated charging based on the proposed SLM are shown.

Impact of Random Uncoordinated PEV Charging:

Results for randomly uncoordinated charging following a normal distribution of scheduling over three different time zones are shown in Figs. 6.8-6.16. The best uncoordinated case occurs if charging is randomly distributed over the widest time zone as is shown for 1800h-0800h (Figs. 6.8-6.10). For this scenario, the impact on the system peak is minimized somewhat; however, voltage deviations beyond regulation limits and high system losses still occur for high PEV penetrations (Figs. 6.9-6.10). This PEV charging scenario is unlikely to happen because most vehicles will start plugging in soon after returning home from work until later in the night, with very few PEV charging occurring in the morning hours.

A more realistic scenario is considered by performing uncoordinated PEV charging over narrower time zones with PEVs charging immediately on arrival from work, or, after some fixed delay into the evening. This is investigated in Figs. 6.11-6.13 and Figs. 6.14-6.16 which show the system impacts of random charging distributed across 1800h-0100h and 1800h-2200h, respectively. The situation becomes worse as the system peak rises sharply and broadens due to much of the PEV charging load coinciding with normal system load peaks (Figs. 6.11 and 6.13). This could cause suboptimal generation dispatching with limited spinning reserve to service this new load peak due to PEVs. Severe voltage deviations (>17%), power losses and significant increase in transformer loading can occur as shown in Table 6.6 and Figs. 6.12-6.13 and 6.15-6.16.

Impact of SLM Coordinated PEV Charging:

In order to overcome detrimental performance degradations with uncoordinated PEV charging, coordinated PEV charging based on the proposed SLM algorithm is demonstrated (Figs. 6.20-6.24, Table 6.6). Coordinated PEV charging without and with PEV owner preferred time zone priorities is also considered (Table 6.6).

Compared to the uncoordinated case, a significant improvement in smart-grid performance is achieved.

Most notably, the system demand peak has been reduced which is more favourable from a standpoint of generation dispatch and preventing overloads (e.g., Fig. 6.20 for 47% PEV penetration). Fig. 6.21 indicates the impacts of SLM PEV charging on voltage profile where the unacceptable voltage deviations of 17.15% at the worst bus (Table 6.6) for uncoordinated PEV charging is compensated to less than 10% to be within the regulation limits. However, there is a trade off in that a few PEV subscribers who designated a preferred priority charging time zone were not accommodated in their requested charging zone because the system reached a point where PEV loading caused voltage regulation to be violated. SLM handled these cases by attempting to schedule the PEV owners shifting the violations to a charging time where the system is not under strain, thereby satisfying constraints. This is evident for higher penetration cases as shown in Figs. 6.20 and 6.23. Conversely, after placement of higher priority PEV subscribers, in some cases (Figs. 6.23-6.24) the SLM permitted lower priority PEVs to charge earlier and sometimes ahead of their requested charging time zone because there was available system capacity to do so without violating system constraints.

The improvement in system efficiency with the SLM coordination strategy is evident in Tables 6.6 and 6.7. Energy losses for the high penetration (63%) with SLM are limited to 2.53% of system consumption versus the worst uncoordinated charging scenario with losses of 3.09% of system consumption. Furthermore, peak power losses are limited to less than a third of the worst case random uncoordinated charging as shown in Fig. 6.22.

The SLM coordinated PEV charging also has positive impacts on peak transformer load currents. For many of the uncoordinated random charging scenarios (Table 6.6), distribution transformers experience load currents of up to 0.88 pu. With SLM coordination, transformer currents are reduced to levels of approximately 0.45 pu.

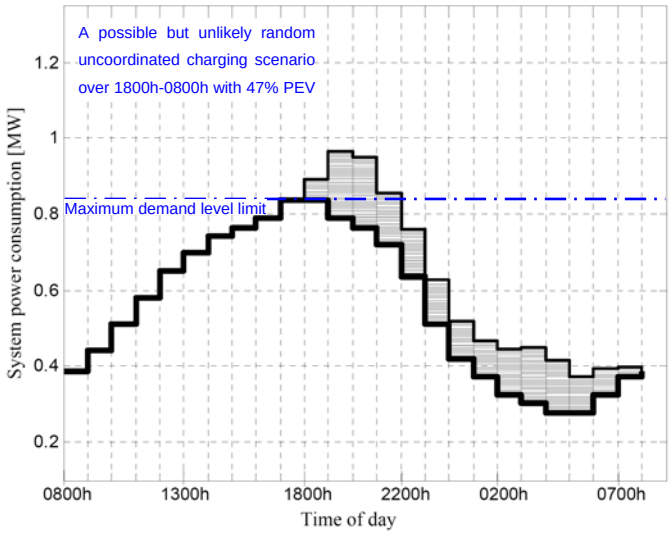

Fig. 6.8. Impact of randomly uncoordinated PEV charging (47% penetration) within green charging zone (1800h-0800h) on the total system power demand

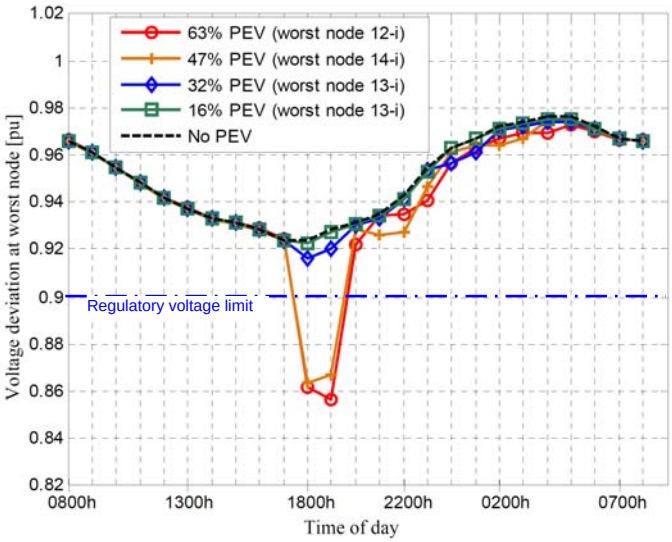

Fig. 6.9. Impact of randomly uncoordinated PEV charging within red zone (1800h-2200h) on voltage profile (shown for worst affected nodes). High PEV penetrations (e.g., >32%) cause considerable voltage deviations.

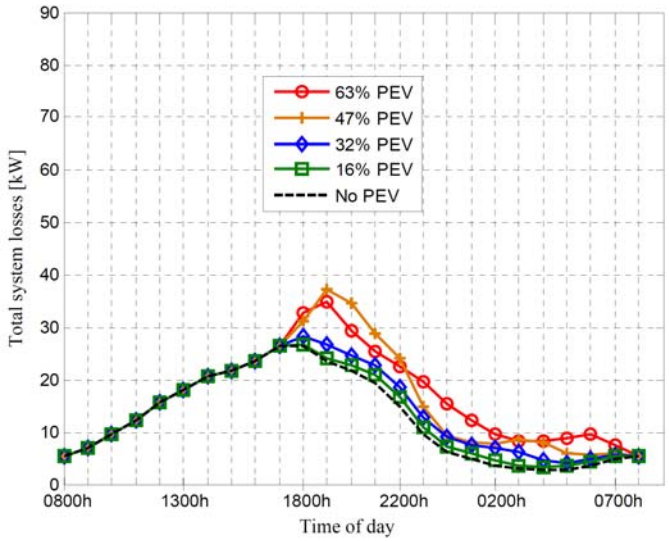

Fig. 6.10. Impact of randomly uncoordinated PEV charging within red zone (1800h-2200h) on the total system power losses

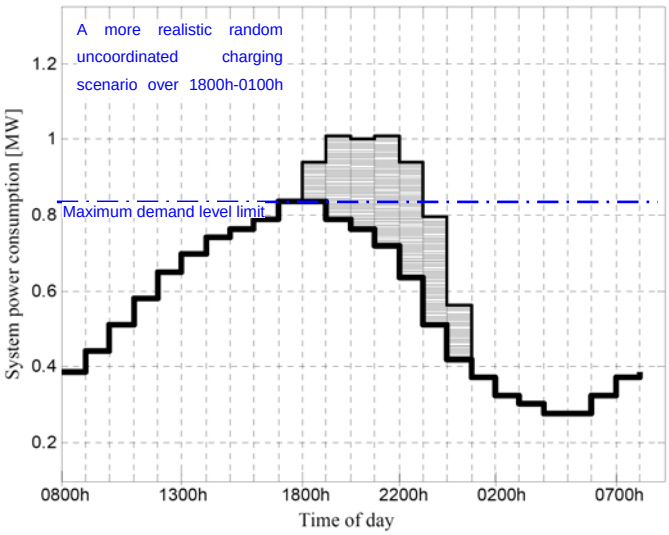

Fig. 6.11. Impact of randomly uncoordinated PEV charging (47% penetration) within blue charging zone (1800h-0100h) on the total system power demand.

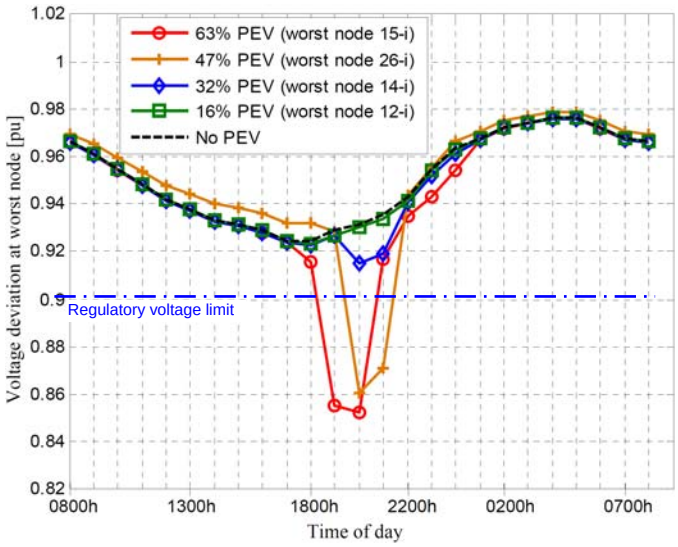

Fig. 6.12. Impact of randomly uncoordinated PEV charging within blue zone (1800h-0100h) on voltage profile (shown for worst affected nodes). High PEV penetrations (e.g., >32%) cause considerable voltage deviations.

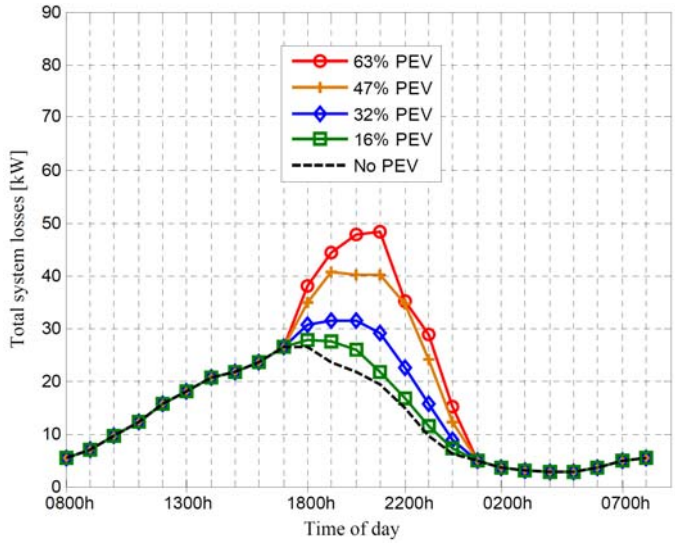

Fig. 6.13. Impact of randomly uncoordinated PEV charging within blue zone (1800h-0100h) on the total system power losses

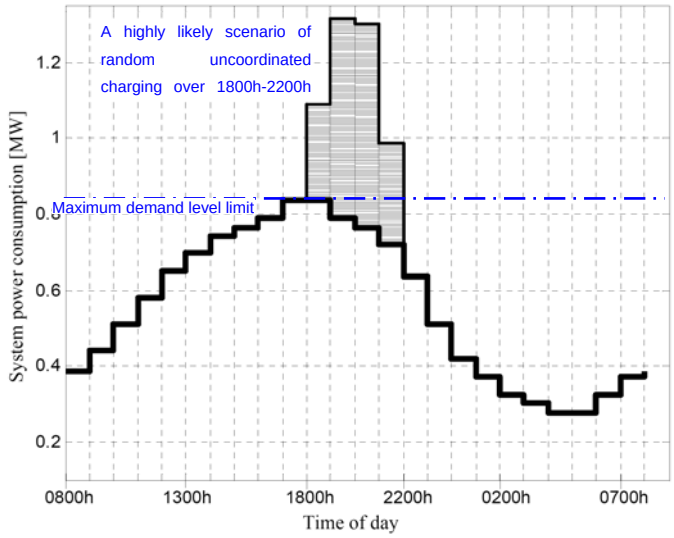

Fig. 6.14. Impact of randomly uncoordinated PEV charging on system load profile for 47% penetration of PEVs over red time zone

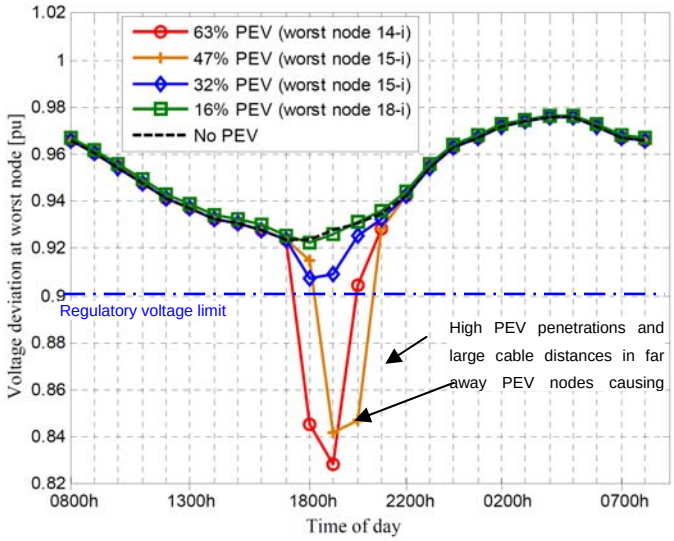

Fig. 6.15. Impact of randomly uncoordinated PEV charging across red zone (1800h-2200h) on voltage profile (shown for worst affected nodes). High PEV penetration (e.g., more than 32%) result in large voltage deviations.

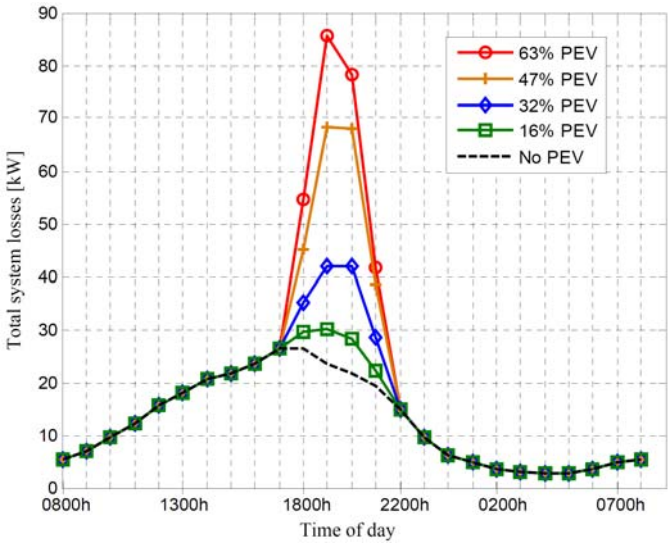

Fig. 6.16. Impact of randomly uncoordinated PEV charging across red zone (1800h-2200h) on total system power losses

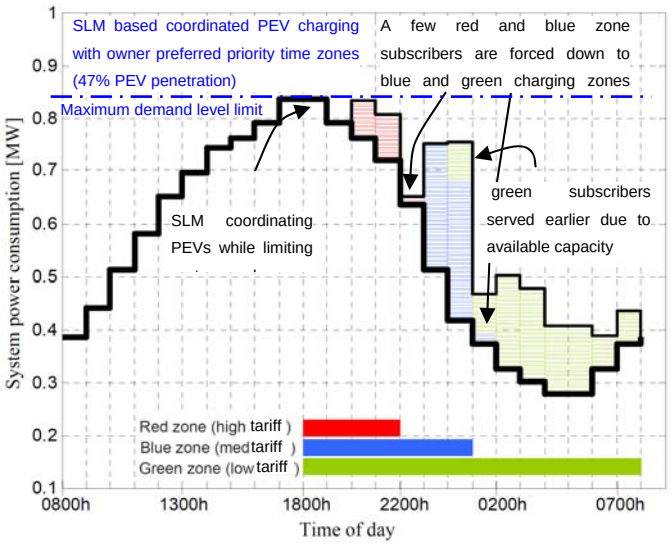

Fig. 6.17. Impact of SLM coordinated PEV charging (47% penetration) on the total system power demand. Note that SLM schedules PEVs in owner designated time zones and minimizes total system peak demand.

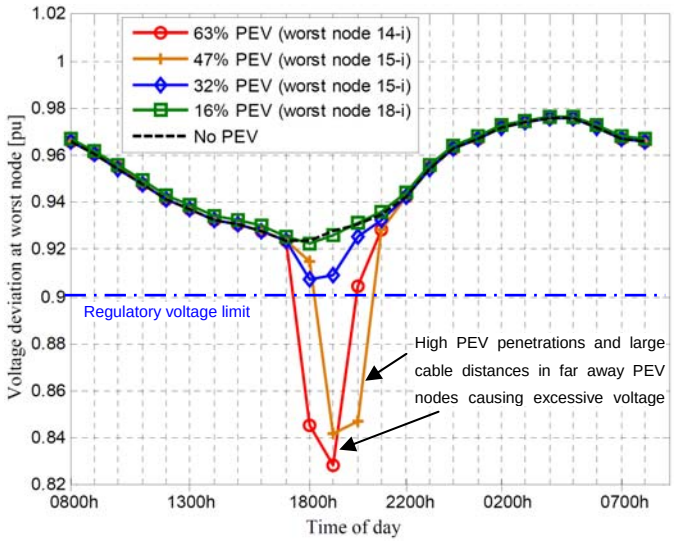

Fig. 6.18. Impact of randomly uncoordinated PEV charging across red zone (1800h-2200h) on voltage profile (shown for worst affected nodes). High PEV penetration (e.g., more than 32%) result in large voltage deviations.

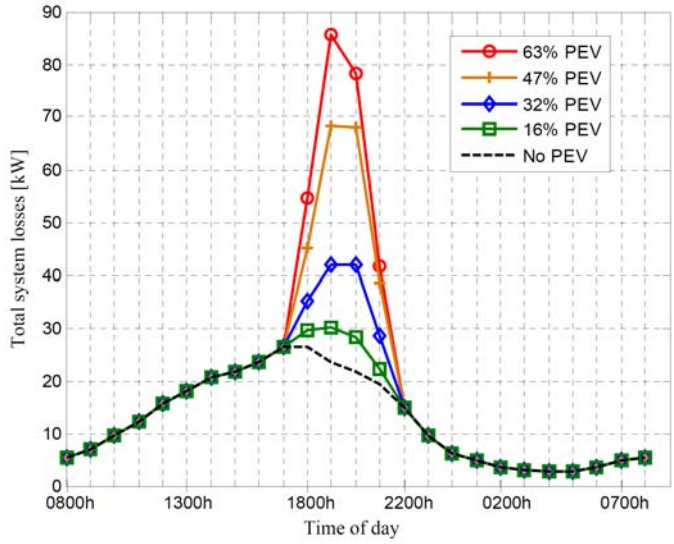

Fig. 6.19. Impact of randomly uncoordinated PEV charging across red zone (1800h-2200h) on total system power losses

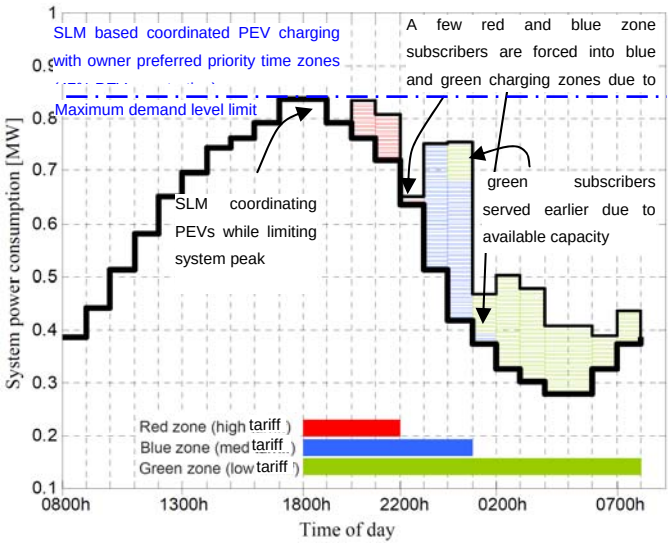

Fig. 6.20. Impact of SLM coordinated PEV charging (47% penetration) on the total system power demand. Note that SLM schedules PEVs in owner designated time zones and minimizes total system peak demand.

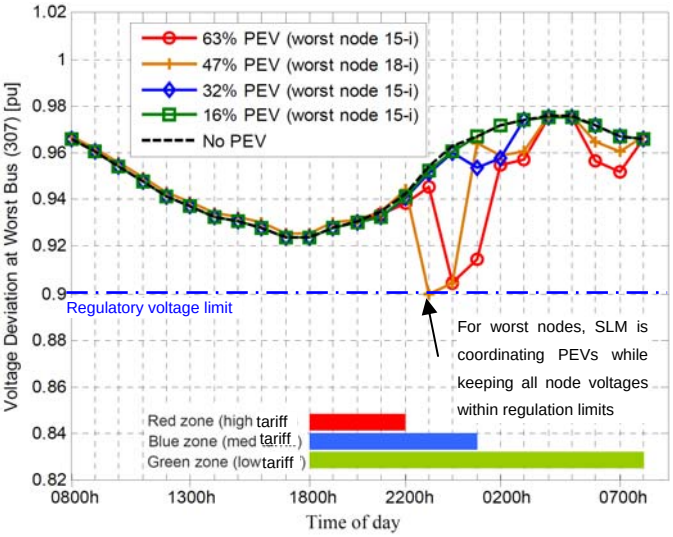

Fig. 6.21. Impact of SLM coordinated PEV charging on voltage profile (shown for affected worst nodes) considering PEV owner priority charging zones. Note that SLM maintains the voltages at all nodes within regulation.

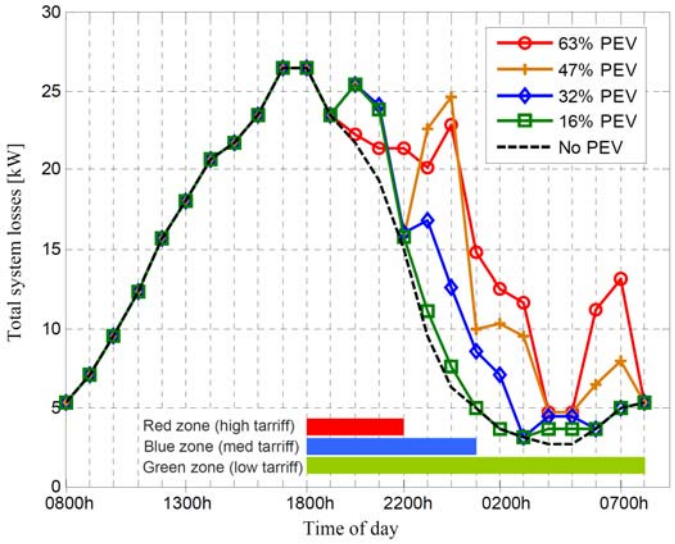

Fig. 6.22. Impact of SLM coordinated PEV charging on total system power losses considering PEV owner priority charging zones. Note the significant reduction in losses compared to uncoordinated random charging.

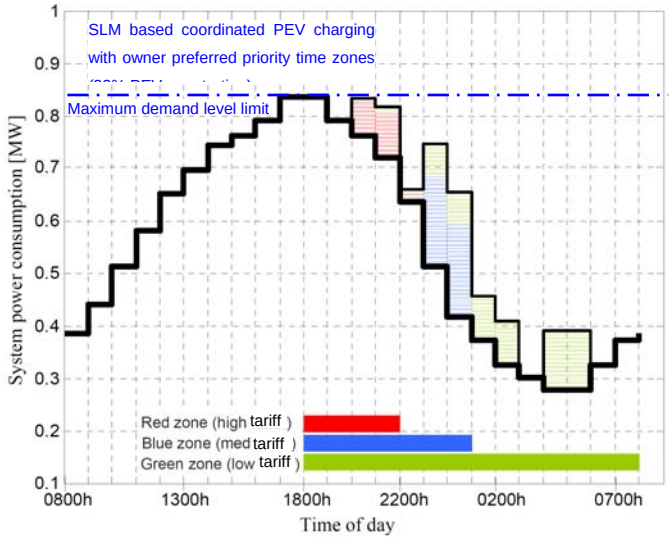

Fig. 6.23. Impact on system power demand with 32 % penetration of PEVs using SLM coordinated PEV charging

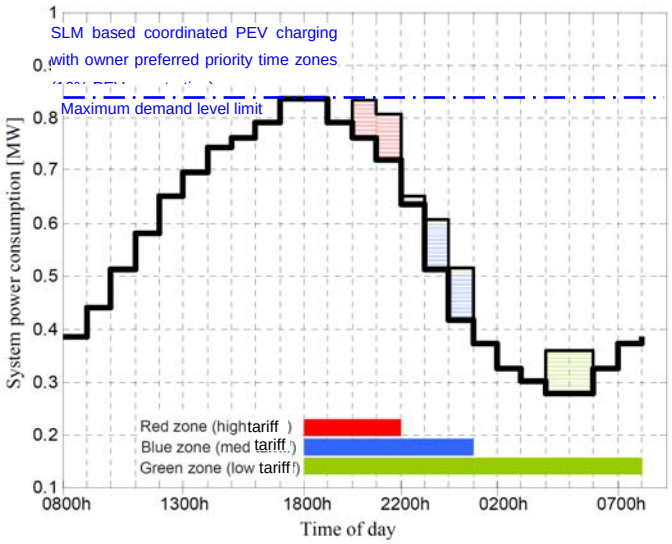

Fig.6.24. System power demand with 16 % penetration of PEVs using SLM coordinated PEV charging

Table 6.6
Impact of uncoordinated and coordinated PEV charging on the power quality of smart grid distribution system (Figure 6.7)

	PEV penetration	UNCOORDINATED CHARGING (RANDOM CHARGING)			SLM COORDINATED CHARGING BASED ON LOSS MINIMIZATION (EQS. 6.1-6.3)		
		Δloss* [%]	ΔV** [%]	I_{MAX}*** [%]	Δloss* [%]	ΔV** [%]	I_{MAX}*** [%]
CASE 1: NO PRIORITY, CHARGING PERIOD: 6PM-8AM (FIGS. 5-7)	16%	2.3141	7.7242	0.47831	2.2939	7.646	0.44071
	32%	2.3818	8.3553	0.52900	2.3411	7.646	0.44071
	47%	2.6188	13.6146	0.60348	2.4936	8.7893	0.44071
	63%	2.6184	14.3304	0.58385	2.4921	9.1211	0.44071
CASE 2: NO PRIORITY, CHARGING PERIOD: 6PM-1AM (FIGS. 8-10)	16%	2.3401	7.6984	0.52591	2.3149	7.646	0.44071
	32%	2.4712	8.5243	0.57259	2.4172	7.7832	0.45499
	47%	2.7659	13.9102	0.64256	2.5737	9.7039	0.45872
	63%	2.8706	14.7455	0.68842	2.6217	9.7946	0.49038
CASE 3: NO PRIORITY, CHARGING PERIOD: 6PM-10PM (FIGS. 11-13)	16%	2.3553	7.8499	0.5546	2.3332	7.646	0.47243
	32%	2.5312	9.2298	0.64324	2.4048	7.646	0.47243
	47%	2.9263	15.8182	0.77095	2.5849	10	0.51682
	63%	3.089	17.1467	0.88626	2.5963	9.9996	0.54002

*) Ratio of system losses over 24 hours compared to total power consumption over 24 hours.
**) Voltage deviation (e.g., 1pu) at the worst bus,
***) Maximum of all distribution transformer load current.

Table 6.7
Impact of coordinated PEV charging based on SLM on the power quality of smart- grids distribution system (Figure 6.7)

PEV penetration	SLM COORDINATED CHARGING BASED ON LOSS MINIMIZATION (EQS. 6.1-6.3, FIGS. 6.14-6.19)		
	Δloss [%]	ΔV [%]	I_{MAX} [%]
16%	2.3192	7.646	0.44071
32%	2.3709	7.646	0.45477
47%	2.5202	9.9958	0.44071
63%	2.5296	9.5615	0.45032

6.3.6. Conclusions

In this study the impact of various random (uncoordinated) charging scenarios as well as coordinated PEV charging are presented. A novel Smart Load Management (SLM) algorithm is developed to improve smart grid performance with high penetration of PEVs. The improvement and benefits of SLM are compared and demonstrated by performing simulations for a highly detailed distribution system topology with several low-voltage residential networks populated with PEVs. Three charging time zones, four PEV penetration levels and three PEV owner's priorities are considered. SLM takes into consideration existing load variations over a 24 hour cycle while factoring PEV owner preferences for charging time zone and priority. The main conclusions are:

- SLM offers a new and viable integrated means of exercising (semi)automated customer demand side management in smart grids, jointly achieving reduced peak demand, improved system efficiency and voltage regulation.
- A feasible pricing and time zone priority scheme is demonstrated and shown to work effectively with SLM PEV charging coordination.
- SLM is shown to be beneficial in limiting overall system overloads as well as reducing the burden on local distribution circuits (e.g., cables and transformers). Therefore, the risk and cost of premature failure of transformers and associated outages can be minimized.

- The impact of PEV was the focus of this study; however, the SLM approach is applicable of coordinating a wider range of loads (e.g., PEV charging stations and smart appliances).
- SLM could be adapted to function with soon to come smart meters as inputs in lieu of load flow to determine system performances necessary for SLM PEV coordination.

The results obtained through the SLM approach are vital for smart-grid reinforcement by improving the reliability and security of the supply to the customer.

CHAPTER SEVEN
SUMMARY AND CONCLUSIONS

In this thesis, the optimization of distorted distribution systems including different types of nonlinear loads have been performed by means of optimal dispatch of load tap changer (LTC) and switched shunt capacitors. For the first time, an ant colony algorithm (ACA) is suggested to solve the problem. The proposed ACA is implemented and tested on a number of IEEE distribution systems including a 449-bus smart grid configuration with plug-in electric vehicles populating the residential feeders. Two additional intelligent dispatch solutions based on GA and Fuzzy-GA are also implemented to evaluate the performance of the ACA in achieving optimization goals and satisfying problem constraints. Simulation results indicate that the objectives of the optimization scheme have been successfully met and the associated constraints have been fully satisfied. In addition, ACA facilities considerable improvements in regulating voltages, reducing power losses and mitigating harmonic distortions. The optimization results can now be summarized by pointing out the research outcomes indicating the contributions of this research. In addition, some suggestions for future research are presented based on the results.

7.1. Thesis Contributions

The main contributions of this research can be summarized as follows:

- The development and testing of ant colony algorithms (ACAs) and their application to optimal dispatch of LTC and shunt capacitor banks considering harmonic distortions. The AC optimization has been recently applied to the optimal dispatch problem under sinusoidal operating conditions; however, the presence of nonlinear loads and the impact of harmonics in the distribution system have not been considered.

- Validation and comparison of the proposed ACA with the recently developed GA and Fuzzy-GA dispatch approaches in terms of optimization benefits (e.g., loss minimization, voltage improvement and THDv reduction), convergence and the required computing time. Based on the simulation results for the modified IEEE 31-bus and 123-bus with the inclusion of nonlinear loads, the three intelligent

algorithms can achieve the optimization objective and fulfill the designated voltage, THDv and switching constraints. However, ACA has better convergence characteristics and requires less computing time to capture the near-global optimal solution.

- Application of the proposed ACA to the optimal dispatch problem in smart-grid distribution and residential systems with PEV charging activities. This research makes an approximation by considering the harmonic distortions of PEV chargers at the distribution level.
- Development and testing of a new smart load management (SLM) algorithm for optimization of smart-grid populated with randomly charging PEVs in low-voltage residential feeders. Coordination of PEV charging is performed for loss minimization over the 24 hours period considering voltage regulation limits.

7.2. Conclusions

The main conclusions of this thesis may be pointed out as follows:

- The optimal scheduling of LTC and shunt capacitors is considered to be a significant method in distribution system operation that enables simultaneously minimizing energy loss, improving voltage profile and power quality.
- The proposed ACA, as well as the recently implemented GA and Fuzzy-GA are suitable for optimal dispatch of LTC and shunt capacitors in the presence of harmonics. They enable the simultaneous scheduling of controllable devices while checking the fulfillment of switching constraints prior to performing unnecessary calculations. This will significantly reduce computation time.
- The three intelligent algorithms perform better than ad-hoc placements of reactive power sources but differ in convergence, computational effort and accuracy of solutions.
- Compared with GA and GA-Fuzzy, the developed ACA results in a slightly better quality of solution in terms of the convergence, voltage profile and THD reduction.

- The generated optimal schedules confirm that the switching constraints that are difficult to be satisfied using other methods, can be effectively achieved based on the ACA.
- The developed ACA can successfully mitigate voltage THDv distortions below the IEEE-519 and IEC-61000 recommended level of 5%, keeps voltage variations at all buses within the designated levels (0.95 and 1.05pu) and reduces power losses.
- ACA can also be utilized in smart-grid systems to improve power quality and voltage profile.
- The proposed SLM offers a new and viable integrated means of exercising (semi)automated customer-demand-side management in smart grids, jointly achieving reduced peak demand, improved system efficiency and voltage regulation.
- SLM achieves performance improvement functions such as loss minimization while maintaining voltage regulation. SLM will respect PEV owner designated charging time zones as long as system constraints are not violated.
- SLM is shown to be beneficial in limiting overall system overloads as well as reducing the burden on local distribution circuits (e.g., cables and transformers). Therefore, the risk and cost of premature failure of transformers and associated outages can be minimized.
- The results obtained through the SLM approach are vital for smart-grid reinforcement by improving the reliability and security of the supply to the customer.

7.3. Future Work

Future work in this field may be performed by considering the following issues:

1. The computation time is crucial in the optimal dispatch problems under non-sinusoidal operating conditions. Therefore, other efficient methods and algorithms with better convergence characteristics such as Hybrid ACA should be investigated.

2. Premature convergence is a common and important problem which may affect optimization methods including ACA and GA techniques. Therefore, their impact on the performance of the optimization methods should not be underestimated. This issue should be further investigated and resolved.
3. Applications and performances of other intelligent approach such as ACA-GA or ACA-Fuzzy should be targeted for smart-grid applications.
4. The impact of PEV was the focus of this study; however, the SLM approach is applicable of coordinating a wider range of loads (e.g., PEV charging stations and smart appliances).
5. SLM could be adapted to function with soon to come smart meters as inputs in lieu of load flow to determine system performances necessary for SLM-PEV coordination.
6. Evolutionary approaches such as genetic algorithm (GA) can be used to perform better coordination of PEVs.
7. Smart appliances and home-area networks should be in included in SLM.
8. Distributed generations such as photovoltaic systems and wind power should be included in the load flow and SLM optimization algorithm.

REFERENCES

Every reasonable effort has been made to acknowledge the owners of copyright material. I would be pleased to hear from any copyright owner who has been omitted or incorrectly acknowledged.

[1]A. Ulinuha, M.A.S. Masoum, and S.M. Islam, "Optimal scheduling of LTC and shunt capacitors in large distorted distribution systems using evolutionary-based algorithms," IEEE Trans. on Power Delivery, vol. 23, no.1, pp.434-441, Jan 2008.

[2]A. Ulinuha, M. A. S. Masoum and S. M. Islam, "Hybrid genetic-fuzzy algorithm for Volt/Var/THD control of distribution systems with high penetration of nonlinear loads'", IET Trans. on Generation, Transmission & Distribution, Paper number: GTD-2010-0168, Under second review.

[3] Y. Baghzouz and S. Ertem, "Shunt capacitor sizing for radial distribution feeders with distorted substation voltage, " IEEE Trans. on Power Delivery, vol. 5, no. 2, pp. 650-657, 1990.

[4]A. Ulinuha, M. A. S. Masoum, and S. M. Islam, "The Accuracy and Efficiency Issues of Decouple Approach for Harmonic Power Flow Calculation, " in Regional Postgraduate Conference on Engineering and Science (RPCES) Johor Bahru, Malaysia, 2006, pp. 213 - 218.

[5]S. Deilami, A.S. Masoum, P.S. Moses, and M.A.S. Masoum, "Demand side management of plug-in electric vehicles in smart grids to minimize power losses and improve voltage profile," Paper number TSG-00112-2010, Submitted to IEEE Trans. on Smart Grid, under second review.

[6]M. Dorigo, "Optimization, learning and natural algorithms," Ph.D. Dissertation, Politecnico de Milano, Milan, Italy, 1992.

[7]M.E. Baran and M.-Y. Hsu, "Volt/VAr control at distribution substations," IEEE Transactions on Power Systems, vol. 14, pp. 312-318, 1999.

[8]R.-H. Liang and C.-K. Cheng, "Dispatch of main transformer ULTC and capacitors in a distribution system," IEEE Transactions on Power Delivery, vol. 16, pp. 625-630, 2001.

[9]R.-H. Liang and Y.-S. Wang, "Fuzzy-based reactive power and voltage control in a distribution system," IEEE Transactions on Power Delivery, vol. 18, pp. 610-618, 2003.

[10]J.J. Grainger and S. Civanlar, “Volt/var control on distribution systems with lateral branches using shunt capacitors and voltage regulators. Part III: The numerical result.” IEEE Transactions on Power Apparatus and Systems, vol. 104, pp. 3291-3297, 1985.

[11]J. J. Grainger and S. Civanlar, “Volt/var control on distribution systems with lateral branches using shunt capacitors and voltage regulators. Part I: The overall problem,” IEEE Transactions on Power Apparatus and Systems, vol. 104, pp. 3278-3283, 1985.

[12]F.-C. Lu and Y.-Y. Hsu, “Fuzzy dynamic programming approach to reactive power/voltage control in a distribution substation,” IEEE Transactions on Power Systems, vol. 12, pp. 681-688, 1997.

[13]Y.-Y. Hsu and F.-C. Lu, “A combined artificial neural network-fuzzy dynamic programming approach to reactive power/voltage control in a distribution substation,” IEEE Transactions on Power Systems, vol. 13, pp. 1265-1271, 1998.

[14]Y. Deng and X. Ren, “Fuzzy modeling of capacitor switching for radial distribution systems, ” in IEEE Power Engineering Society Winter Meeting, vol. 2, pp. 830-834, 2001.

[15]Y. Deng, X. Ren, C. Zhao, and D. Zhao, “A heuristic and algorithmic combined approach for reactive power optimization with time-varying load demand in distribution systems, ” IEEE Transactions on Power Systems, vol. 17, pp. 1068-1072, 2002.

[16]I. Roytelman, B. K. Wee, and R. L. Lugtu, “Volt/var control algorithm for modern distribution management system, ” IEEE Transactions on Power Systems, vol. 10, pp. 1454-1460, 1995.

[17]G. Ramakrishna and N. D. Rao, “Fuzzy inference system to assist the operator in reactive power control in distribution systems,” IEE Proceedings-Generation, Transmission and Distribution, vol. 145, pp. 133-138, 1998.

[18]G. Ramakrishna and N. D. Rao, “Adaptive neuro-fuzzy inference system for volt/var control in distribution systems,” Electric Power Systems Research, vol. 49, pp. 87-97, 1999/3/1 1999.

[19]F.-C. Lu and Y.-Y. Hsu, “Reactive power/voltage control in a distribution substation using dynamic programming,” IEE Proceedings-Generation, Transmission and Distribution, vol. 142, pp. 639-645, 1995.

[20]Z. Gu and D. T. Rizy, “Neural networks for combined control of capacitor banks and voltage regulators in distribution systems,” IEEE Transactions on Power Delivery, vol. 11, pp. 1921-1928, 1996.

[21]G. Ramakrishna and N. D. Rao, “Implementation of a fuzzy logic scheme for Q/V control in distribution systems,” IEEE Power Engineering Society Winter Meeting, vol.2, pp. 1316-1321, 1999.

[22]J.J. Grainger and S. Civanlar, “Volt/var control on distribution systems with lateral branches using shunt capacitors and voltage regulators. Part II: The solution method,” IEEE Transactions on Power Apparatus and Systems, vol. 104, pp. 3284-3290, 1985.

[23]Z.Q. Wu and K.L. Lo, “Optimal choice of fixed and switched capacitors in radial distributors with distorted substation voltage,” IEE Proceedings-Generation, Transmission and Distribution, vol. 142, no. 1, pp. 24-28, 1995.

[24]Y. Liu, P. Zhang, and X. Qiu, “Optimal reactive power and voltage control for radial distribution system, ” in Power Engineering Society Summer Meeting, pp. 85-90, 2000.

[25]Y. Liu, P. Zhang, and X. Qiu, “Optimal volt/var control in distribution systems,” International Journal of Electrical Power & Energy Systems, vol. 24, pp. 271-276, 2002/5 2002.

[26]R. Baldick and F. F. Wu, “Efficient integer optimization algorithms for optimal coordination of capacitors and regulators,” IEEE Transactions on Power Systems, vol. 5, pp. 805-812, 1990.

[27]M.A. S. Masoum, P. S. Moses, and S. Deilami, “Load management in smart grids considering harmonic distortion and transformer derating, ” in International Conference on Innovative Smart Grid Technologies (ISGT), 2010, pp. 1-7.

[28]A.F. Zobaa,“A new approach for voltage harmonic distortion minimization,” Electric Power Systems Research, vol. 70, no. 3, pp. 253-260, 2004.

[29]A.F. Zobaa and M.M. Aziz, “LC compensators based on transmission loss minimization for nonlinear loads,” IEEE Transactions on Power Delivery, vol. 19, no. 4, pp. 1740-1745, 2004.

[30]M. A. S. Masoum, M. Ladjevardi, A. Jafarian, and E. F. Fuchs, “Optimal placement, replacement and sizing of capacitor banks in distorted distribution networks by genetic algorithms,” IEEE Transactions on Power Delivery, vol. 19, no. 4, pp. 1794-1801, 2004.

[31]M. A. S. Masoum, A. Jafarian, M. Ladjevardi, E. F. Fuchs, and W. M. Grady, "Fuzzy approach for optimal placement and sizing of capacitor banks in the presence of harmonics," IEEE Transactions on Power Delivery, vol. 19, no. 2, pp. 822 - 829, 2004.

[32]M. A. S. Masoum, M. Ladjevardi, E. F. Fuchs, and W. M. Grady, "Application of local variations and maximum sensitivities selection for optimal placement of shunt capacitor banks under nonsinusoidal operating conditions," International Journal of Electrical Power & Energy Systems, vol. 26, no. 10, pp. 761-769, 2004.

[33]M. Dorigo, V. Maniezzo, and A. Colorni, "Ant system: optimization by a colony of cooperating agents," IEEE Trans. Syst., Man, Cybern. B, vol. 26, pp. 29-41, Feb. 1996.

[34]]J.P. Chiou, and C. F. Chang, "Ant direction hybrid differential evolution for solving large capacitor placement problems," IEEE Trans. Power Systems, vol. 19, no. 4, pp.1794-1800, November 2004.

[35]C.F. Chung, "Reconfiguration and capacitor placement for loss reduction of distribution systems by ant colony search algorithm," IEEE Trans. Power Apparatus and Systems, vol. 23, no. 4, November 2008.

[36]J.G. Vlachogiannis, and N. D. Hatziargyriou, "Ant colony system-based algorithm for constrained load flow problem," IEEE Trans. Power Systems, vol. 20, no. 3, pp. 1241-1249, August 2005.

[37]M. Dorigo, M. Birattari, and T. Stutzle, "Ant colony optimization," IEEE Computational Inteligence Magazine, vol. 1, no.4, pp.28-39, 2006.

[38]A. Abbasy and S.H. Hosseini, "Ant colony optimization-based approach to optimal reactive Power dispatch: a comparison of various ant systems", IEEE PES Power Africa, pp.1-8, 2007.

[39]M. Dorigo and L. M. Gambardella, "ant colony system: a cooperative learning approach to the travelling salesman problem," IEEE Trans. Evol. Comput. vol. 1, no. 1, pp. 53–66, Apr. 1997.

[40]A. Ulinuha, M. A. S. Masoum, and S. M. Islam, "Decoupled harmonic power flow for large power system with multiple nonlinear loads," in The Seventh Postgraduate Electrical Engineering and Computing Symposium (PEECS), Perth, Australia, 2006.

[41]A. Ulinuha, M. A. S. Masoum, and S. M. Islam, "harmonic power flow calculations for large power system with multiple nonlinear loads using decouple approach," in

Australasian Universities Power Engineering Conference (AUPEC), Perth, Australia, 2007.

[42]Yu, X.-M., Xiong, X.-Y., Wu, and Y.-W, "A PSO-based approach to optimal capacitor placement with harmonic distortion consideration," Electric Power Systems Research, vol.1, pp. 27-33, 2004.

[43]J.H. Holland, "Adaptation in natural and artificial systems," University of Michigan Press, Ann Arbor 1975.

[44]D. E. Goldberg, "Genetic algorithms in search, optimization, and machine learning," Massachusetts: Addison-Wesley Publishing Company, Inc., 1953.

[45]A. El-Habachi, "Optimal planning of distribution system harmonics," in IEEE Power Engineering Society Summer Meeting, pp. 433-437, 2002.

[46]Z. Michalewics, "Genetic algorithms + data structures = evolution program," 3ed. New York: Springer-Verlag Berlin Heidelberg, 1996.

[47]M. Delfanti, G. P. Granelli, P. Marannino, and M. Montagna, "Optimal capacitor placement using deterministic and genetic algorithms, " IEEE Transactions on Power Systems, vol. 15, pp. 1041-1046, Aug 2000.

[48]V. Glamocanin, D. Andonov, D. Trajanov, and B. Stojkovska, "Optimal power system VAr planning by AI algorithm," in Electrotechnical Conference, 1998. MELECON, 9th Mediterranean, Tel-Aviv Israel, 1998, pp. 1066 - 1070.

[49]K. Y. Lee, and F. F. Yang, "Optimal reactive power planning using evolutionary algorithms: a comparative study for evolutionary programming, evolutionary strategy, genetic algorithm, and linear programming," IEEE Transactions on Power Systems, vol. 13, pp. 101-108, Feb 1998 1998.

[50]H. Mori and H.-D. Chiang, "A genetic algorithm-based approach to stochastic Var planning in power systems, " in Proceedings of the 4th IEEE Conference on Control Applications, Albany, NY USA, 1995, pp. 810 - 811.

[51]S. Deilami, M.A.S. Masoum, and S. Islam, "Optimal dispatch of lTC and shunt capacitors in large distribution systems considering harmonic distortion using ant colony system", IET on Generation, Transmission and Distribution, under review.

[52]D.T. Pham and D. Karaboga, "Intelligent optimisation technique: genetic algorithms, tabu search, simulated annealing and neural network," London: Springer-Verlag, 1998.

[53]A.L. Shenkman, “Energy loss computation by using statistical techniques,” IEEE Transactions on Power Delivery, vol. 5, pp. 254-258, 1990.

[54]E.F. Fuchs and M.A.S. Masoum, “Power quality and power systems in electrical machines,” New York: Academic, 2008.

[55]J.A. Orr, A.E. Emanuel and K.W. Oberg, “Current harmonics generated by a cluster of electric vehicle battery chargers,” IEEE Trans. Power App. Syst., no. 3, pp. 691–700, March 1982.

[56]M.A.S. Masoum, P. Moses and S. Deilami, “Load management in smart grids considering harmonic distortion and transformer derating,” 2010 IEEE PES Conference on Innovative Smart Grid Technologies, Jan 19-21, 2010.

[57]P. T. Staats, W. M. Grady, A. Arapostathis, and R. S. Thallam, “A statistical method for predicting the net harmonic currents generated by a concentration of electric vehicle battery chargers,” IEEE Trans. Power Del., vol. 12, no. 3, pp. 1258–1266, July 1997.

APPENDIX A

LIST OF THE SUPPORTING PAPERS

1. S. Deilami, A.S. Masoum, P.S. Moses, M.A.S. Masoum, "Voltage Profile and THD Distortion of Residential Network with High Penetration of Plug-in Electrical Vehicles", IEEE ISGT Europe 2010 (Innovative Smart Grid Technologies Europe) conference, Gothenburg, Sweden, pp. 1-6, October 10-13, 2010.

2. P.S. Moses, S. Deilami, A.S. Masoum, M.A.S. Masoum, "Power Quality of Smart Grids with Plug-in Electric Vehicles Considering Battery Charging Profile", IEEE ISGT Europe 2010 (Innovative Smart Grid Technologies Europe) conference, Gothenburg, Sweden, pp. 1-6, October 10-13, 2010.

3. A.S. Masoum, S. Deilami, P.S. Moses, A. Abu-Siada, "Impacts of Battery Charging Rates of Plug-in Electric Vehicle on Smart Grid Distribution System", IEEE ISGT Europe 2010 (Innovative Smart Grid Technologies Europe) conference, Gothenburg, Sweden, pp. 1-6, October 10-13, 2010.

4. M.A.S. Masoum, Sara Deilami, S. Islam, "Mitigation of Harmonics in Smart Grids with High Penetration of Plug-In Vehicles", IEEE Power Engineering Society General Meeting, Minneapolis, USA, pp. 1-8, July, 2010.

5. M.A.S. Masoum, P. Moses, S. Deilami, "Load Management in Smart Grids Considering Harmonic Distortion and Transformer Derating", IEEE ISGT 2010 (Innovative Smart Grid Technologies) conference, Gaithersburg, Maryland, USA, pp. 1-7, Jan. 19-21, 2010.

6. A.S. Masoum, S. Deilami, P.S. Moses, A. Abu-Siada, "Impact of Plug-in Electrical Vehicles on Voltage Profile and Losses of Residential," Australasian Universities Power Engineering Conference (AUPEC 2010), Dec. 5-8, 2010, Christchurch, New Zealand, Accepted for presentation and publication (Paper No: 101).

7. A.S. Masoum, S. Deilami, P.S. Moses, M.A.S. Masoum, A. Abu-Siada, "Smart Load Management of Plug-In Electric Vehicles in Distribution and Residential Networks with Charging Stations for Peak Shaving and Loss Minimization Considering Voltage Regulation", Paper number GTD-2010-057, IET on Generation, Transmission and Distribution, accepted for publication.

8. MS. Deilami, M.A.S. Masoum, S. Islam, “Optimal Dispatch of LTC and Shunt Capacitors in Large Distribution Systems considering harmonic distortion using Ant Colony System”, IET on Generation, Transmission and Distribution, under review.